2014

Omniphobic "RF Paper" Produced by Silanization of Paper with Fluoroalkyltrichlorosilanes

Ana C. Glavan, *Harvard University*
Ramses V. Martinez, *Harvard University*
Anand Bala Subramaniam, *Harvard University*
Hyo Jae Yoon, *Harvard University*
Rui M.D. Nunes, *Harvard University*, et al.

Submitted to ADVANCED FUNCTIONAL MATERIALS

DOI: 10.1002/adfm. XXX.

Omniphobic "R^F Paper" Produced by Silanization of Paper with Fluoroalkyltrichlorosilanes

By *Ana C. Glavan*[1], *Ramses V. Martinez*[1†], *Anand Bala Subramaniam*[1†], *Hyo Jae Yoon*[1], *Rui M.D. Nunes*[1], *Heiko Lange*[1], *Martin M. Thuo*[1], *and George M. Whitesides*[1,2*]

[*] Prof. G. M. Whitesides
[1] Department of Chemistry and Chemical Biology, Harvard University, 12 Oxford Street, Cambridge, MA 02138, (USA).
[2] Wyss Institute for Biologically Inspired Engineering, Harvard University, 60 Oxford Street, Cambridge, MA 02138, (USA).
E-mail: gwhitesides@gmwgroup.harvard.edu

A. C. Glavan, Dr. R. V. Martinez, Dr. A. B. Subramaniam, Dr. H. J. Yoon, Dr. R. M. D. Nunes, Dr. H. Lange, Dr. M. M. Thuo
[1] Department of Chemistry and Chemical Biology, Harvard University, 12 Oxford Street, Cambridge, MA 02138, USA.

(†) Authors have contributed equally to this work.

Keywords: Omniphobic Paper, SLIPS, Paper SLIPS, Origami, Hydrophobic Paper.

Abstract

This paper describes the fabrication and properties of "fluoroalkylated paper" ("R^F paper") by vapor-phase silanization of paper with fluoroalkyl trichlorosilanes. R^F paper is both hydrophobic and oleophobic: it repels water ($\theta_{app}H_2O$ >140°), organic liquids with surface tensions as low as 28 mN/m, aqueous solutions containing ionic and non-ionic surfactants, and complex liquids such as blood (which contains salts, surfactants, and biological material such as cells, proteins, and lipids). The propensity of the paper to resist wetting by liquids with a wide range of surface tensions correlates (with a few exceptions) with the length and degree of fluorination of the organosilane, and with the roughness of the paper. R^F paper

maintains the high permeability to gases, and the mechanical flexibility of the untreated paper, and can be folded into functional shapes (e.g. microtiter plates and liquid-filled gas sensors). When impregnated with a perfluorinated oil, R^F paper forms a "slippery" surface (paper slippery liquid-infused porous surface, or "paper SLIPS") capable of repelling liquids with surface tensions as low as 15 mN/m. The foldability of the paper SLIPS allows the fabrication of channels and flow switches to guide the transport of liquid droplets.

1. Introduction

The design of devices that handle liquids, or control the transport of gases, would benefit from new materials, and from repurposing currently available materials to have new properties and functions. To channel or restrict the flow of liquids requires non-permeable materials; to transport gases requires porous media. Porous, water-repellent materials based on expanded polytetrafluoroethylene (ePTFE, Gore-Tex®, Nafion®, Teflon®) and other polymers have been useful in a wide range of applications, from high performance fabrics and membrane filters to fuel cells,[1] surgical implants[2-5] and lung-assist devices.[6, 7] The relatively high cost (from ~\$1500/m^2 for Nafion® to ~ \$29/m^2 for Gore-Tex®) of these materials has, however, limited their utilization for applications requiring a low-cost or single-use format.

Paper is a useful substrate in applications that require low cost, flexibility, disposability, porosity, and adaptability to large-scale manufacturing.[8-11] In recent years, it has become increasingly popular as a material for the construction of "high-tech" devices in consumer electronics, [12-14] chemical and physical microelectromechanical systems (MEMS) sensors,[8, 15-17] user interfaces,[18] electronic displays,[19] cell-based assays[20] and microfluidic devices.[10, 21] The tendency of paper to absorb solvents (including water), however, limits its adoption as

a substrate in liquid-handling applications in which wicking is not desirable, or in which moisture and humidity can cause deleterious effects (especially changes in mechanical and electrical properties). For such applications, paper must be made resistant to wetting by liquids, and to adsorption of liquids (especially water) from the atmosphere.

This work describes a rapid, simple method for altering the surface chemistry of paper by treatment with organosilanes in the gas phase. Reaction of paper with alkyl trichlorosilanes rendered paper resistant to wetting by high surface tension liquids such as water, while preserving the flexibility and low resistance to the passage of gas of the untreated paper. We compared the wetting behaviors of three papers of different surface roughness—each functionalized with organosilanes of different alkyl chain lengths, and different levels of fluorination—to characterize systematically the contributions of roughness and surface chemistry to the wetting properties of the modified paper.

Treatment of all three papers with fluorinated alkyl trichlorosilanes made them resistant to wetting by both water and non-polar liquids such as n-hexadecane. The "fluoroalkylated paper," or "R^F paper" is thus omniphobic (i.e. both hydrophobic and oleophobic). R^F paper repelled liquids spanning a broader range of surface tensions than paper surfaces treated with non-fluorinated alkyl trichlorosilanes ("non-fluorinated paper", or "R^H paper"), even though both fluorinated and non-fluorinated paper surfaces exhibited similar contact angles with water ($\theta_{app}H_2O$ >140°, where $\theta_{app}H_2O$ is the apparent static contact angle of water on the modified paper). The combined effects of the long fluoroalkyl chains of grafted siloxane molecules with the micro-scale roughness and porosity of paper (typical papers have a ~30-45% void volume), yield an omniphobic material that preserves the properties of mechanical flexibility and low resistance to transport of gas of the untreated paper.

2. Background

We and others have used a variety of techniques to minimize the tendency of paper to adsorb liquids (reviewed here [22-28]). Methods to render paper hydrophobic include spraying alcohol suspensions of SiO_2 nanoparticles on surface of the paper,[29] soaking in polystyrene solutions,[30] patterning using photolithography with SU-8,[10] wax printing,[9] plasma processing,[31] and treatment with silanizing reagents.[8, 32-35]

Organosilanes with hydrophobic organic groups have been used to make the hydrophilic hydroxyl-rich surfaces of cellulose-based materials hydrophobic following both gas-phase[33, 34, 36, 37] and solution immersion reactions.[34, 38-40] Most methods, however, require long reaction and processing times (usually longer than one hour[33, 34]), and immersion in solvents requires pre- or post- treatment steps (washing cycles to remove excess reagents or side products, drying, etc.); these processes typically produce surfaces that have limited hydrolytic stability,[41] or limited repellency to liquids with surface tensions lower than that of water.[33] They also often cause the paper to buckle or warp.

The method we describe transforms paper into an omniphobic material by exposure to vapors of a fluoroalkyl trichlorosilane; it is simple (single step), rapid (~5 min to completion) and low-cost. We estimate a cost for the materials required for the transformation of hydrophilic paper into an omniphobic material to be less than $\$0.8/m^2$ (for materials purchased on a small scale, as research reagents). We characterized the wetting behavior of the R^F paper, and used it to fabricate functional paper-based devices: microtiter plates able to contain polar and non-polar solvents, and gas sensors, both constructed using the principles of origami.[42]

Part of the oleophobicity of organosilane-functionalized paper reflects its textured surface—a mixture of small fibers and voids—which enables it to form metastable composite solid-liquid-air interfaces. This architecture—one comprising voids and solid structures—is the basis of other hydrophobic and omniphobic surfaces[43] and is part of the well-studied lotus leaf effect.[44] Aizenberg et al. and more recently others, have extended this type of structure to sub-micron pillars—etched[45] or molded into a solid support.[46]

A different biomimetic architecture inspired by the *Nepenthes* pitcher plant involves the formation of an immobilized film of a low surface tension liquid at the "solid"-air or "solid"-liquid interface; this structure nearly eliminates pinning of the contact line for both high- and low-surface-tension liquids, and leads to a remarkably low contact angle hysteresis. Based on this principle, the Aizenberg group created omniphobic "slippery" surfaces (SLIPS) from low surface energy porous microstructured solid substrates, such as Teflon membranes or arrays of nanoposts functionalized with polyfluoroalkyl silanes, by infusing them with a perfluorinated oil.[47] Following this lead, we further increased the ability of R^F paper to resist wetting by low surface tension liquids (<15 mN/m), by infusing R^F paper with perfluorinated oils. Paper SLIPS have the advantage of being mechanically flexible, and thus can be folded into three-dimensional structures to serve as elementary flow switches and channels for guided transport of drops of liquid.

3. Results and Discussion

3.1. Fabrication of R^F paper via silanization

We used Whatman chromatography paper as the starting material because it is uniform in structure and free of hydrophobic binders or coatings that could interfere with, or mask, the effect of silanization. We chose three types of papers: Whatman Gel Blot paper, Whatman #1 paper, and Whatman #50 paper (see **Figure 1**c for SEM images). The root mean square surface roughness, $R_{R.M.S.}$ of these papers, as measured by optical profilometry, was $R_{R.M.S.}$=24 ± 1 μm for Gel Blot paper, $R_{R.M.S.}$= 18.0 ± 0.4 μm for Whatman #1 paper, and $R_{R.M.S.}$=14.5± 0.7 μm for Whatman #50 paper.

We chose gas-phase silanization to render paper hydrophobic because the procedure does not require pre- or post- treatment steps and the processing can be completed within minutes. We believe this method, with development, is scalable and compatible with large-scale processing (that is, it will be able to generate virtually unlimited areas of silanized paper, using a standard reel-to-reel processing technique).

We used five commercially available organosilane reagents ($RSiCl_3$), in order to study the effect of chain length and fluorination of the organosilane on the wettability of paper: i) methyltricholorosilane (CH_3SiCl_3, "C_1^H"); ii) decyltrichlorosilane ($CH_3(CH_2)_9SiCl_3$, "C_{10}^H"); iii) (3,3,4,4,5,5,6,6,7,7,8,8,8-tridecafluorooctyl) trichlorosilane ($CF_3(CF_2)_5CH_2CH_2SiCl_3$, "$C_8^F$"); iv) (3,3,4,4,5,5,6,6,7,7,8,8,9,9,10,10,10-heptadecafluorodecyl) trichlorosilane ($CF_3(CF_2)_7CH_2CH_2SiCl_3$, "$C_{10}^F$") ; v) (3,3,4,4,5,5,6,6,7,7,8,8,9,9,10,10, 11,11,12,12,12-henicosafluorododecyl) trichlorosilane ($CF_3(CF_2)_9CH_2CH_2SiCl_3$, "$C_{12}^F$"); C_{12}^F is the trichlorosilane with the longest fluorinated alkyl chain that is commercially available.

The silanization reaction was performed in a vacuum oven at 95 °C and 30 mbar using a solution of the organosilane (~10 mL of a ~30 mM solution in toluene) to supply a useful concentration of the silanizing reagent in the vapor phase. The organosilane was allowed to react with the hydroxyl-rich cellulose paper surfaces for 5 min (this time and temperature are not optimized). This process makes it possible to functionalize the areas of paper (>100 cm^2) required for experimental work rapidly, using low quantities of organosilane and solvent.

3.2. Characterization of the wettability of silanized paper

We examined, by means of apparent static (θ_{app}), advancing (θ_a), and receding (θ_r) contact angle measurements, the wettability of paper substrates modified by gas-phase silanization by a wide range of liquids: organic liquids with different surface tensions, biological fluids, and aqueous solutions of ionic and non-ionic surfactants above the critical micelle concentration (cmc). To ensure that the shape of the droplet is determined by surface forces and is not due to gravitational deformation, we used 10 μL droplets of liquid for the contact angle measurements. For a liquid of density ρ and surface tension $\gamma_{LV,}$ the resulting droplets had radii of ~1.4 mm, below the capillary length λ_c:

$$\lambda_c = \sqrt{\frac{\gamma_{LV}}{\rho g}} \tag{1}$$

For the liquids we selected, λ_c ranged between 1.6 mm (for pentane) and 2.7 mm (for water). In addition, we tested the compatibility of the different silanized papers with buffers relevant for immunoassays,[48-50] electrophoresis,[51-53] magnetic levitation,[54] polymerase chain reactions (PCR),[55, 56] and culture of mammalian cells[57, 58] or bacteria.[59]

r^2

3.3. Treatment of paper with an organosilane (either $R^{H}SiCl_3$ or $R^{F}SiCl_3$) in the vapor phase renders paper highly repellent to pure water

Figure 1a shows that silanization rendered paper highly hydrophobic; water no longer wicked into the paper, but instead formed droplets on the surface with apparent static contact angles, θ_{app}, between 130º and 160º, and with contact angle hysteresis from 7º to 20º. The apparent contact angle of each type of functionalized paper increased (modestly) for the most part with the chain length and degree of fluorination of the organosilane, while the hysteresis did not show any noticeable trends (Figure 1b).

The equilibrium contact angle, $\theta_{Y,}$ that a liquid forms on a chemically homogeneous, smooth solid surface is given by the Young's equation (Equation 2), where γ_{SV} is the solid/vapor surface free energy per unit area, γ_{SL} is the solid/liquid surface free energy per unit area, and γ_{LV} is the liquid/vapor surface free energy per unit area:[60]

$$cos\,\theta_Y = \frac{\gamma_{SV}-\gamma_{SL}}{\gamma_{LV}} \quad (2)$$

From Equation (2) it is apparent that water will form a higher contact angle on surfaces with lower surface free energy, i.e. lower γ_{SV} (even on rough hydrophobic surfaces [60]). Thus, our results can be rationalized, assuming approximately equal grafting densities of the organosilanes on paper, by noting that (i) trifluoromethyl and difluoromethylene groups have a lower energy than methyl and methylene groups,[60] respectively, and that (ii) longer chains lead to more fluorine groups on the surface of the paper. Paper functionalized with methyltrichlorosilane however, consistently exhibited higher static contact angles than what would have been predicted from the properties of the grafted methyl group (Figure 1b). The literature reports that methyltrichlorosilanes can polymerize and form nanoscale three-

dimensional features such as cross-linked nanofibers[61] or nanospheres.[33, 61] On the paper surface, such polymerized features result in a grafting density of methyl siloxanes that is higher than the grafting density of the longer alkyl siloxanes, and could also lead to changes in the topography of the surface.

Since paper is composed of a mesh of partially oriented cellulose fibers, wetting of liquids on its surface is not only dictated by the surface free energy per unit area, but also by the topography of the surface.[60] To account for the topography, Equation (2) must to be modified appropriately. Two models of wetting on "rough" surfaces are widely used, (i) the Wenzel model for homogeneous wetting, with the liquid following the topography of the surface, and (ii) the Cassie-Baxter model, with the liquid droplets exhibiting composite, heterogeneous wetting with air pockets trapped between protruding topographical features. [60]

In the Wenzel model, [62] the apparent contact angle that a liquid droplet makes on the rough surface is given by Equation (3), where r is the non-dimensional substrate "roughness", defined as the ratio of the real surface area to the apparent (projected) area; $r = 1$ for a smooth surface and $r > 1$ for a rough surface.

$$cos\,\theta_{app} = r cos\,\theta_Y \quad (3)$$

When the liquid droplet exhibits composite wetting, i.e. the area wetted consists of liquid-solid contacts and liquid-air contacts (the air being trapped between the troughs of the rough surface) the Cassie-Baxter model, described by Equation (4), is applicable. Here f_1 is the area fraction of the liquid interface in contact with the solid and $f_2=1-f_1$ is the area fraction of the droplet in contact with the air trapped between troughs.

$$cos\,\theta_{app} = r f_1\, cos\,\theta_Y - f_2 \quad (4)$$

In both models, increasing *r* leads to a higher apparent contact angle for hydrophobic ($\theta_Y > 90^o$) surfaces. The geometric parameter *r* however, depends not only on the topography but also on the local contact angle that the liquid makes on the surface features.[43] We assume that the root mean square roughness of the surface ($R_{R.M.S.}$) correlates with *r*. Indeed, our data show that water forms droplets with higher apparent contact angles on surfaces with higher $R_{R.M.S.}$ roughness (Figure 1). The contact angle data of methyltrichlorosilane (C_1^H)-treated paper did not follow the trend, and showed no measurable difference between the different types of paper. We speculate that the nanostructures [33, 61] that form on the paper fibers dominate the wetting of C_1^H-treated papers.

3.4. R^F paper repels a wider variety of liquids than R^H paper

Many applications involve contact of surfaces with liquids that have lower surface tensions than water. To determine the compatibility of silanized paper with organic liquids, we measured the contact angles of nine test liquids with liquid-air interfacial tensions that range from 16 and 83 mN/m on silanized paper (surface tensions obtained from tabulated values in the literature).[63]

R^H paper was able to resist wetting by liquids with surface tensions > 54 mN/m (thiodiglycol; $(HOCH_2CH_2)_2S$). Test liquids with lower surface tensions wicked into the paper. R^F paper was able to resist wetting by liquids with surface tensions as low as 27 mN/m (hexadecane) (**Figure 2** and Supporting Information, Figure S3). This value likely reflects the lower energy of the paper fibers functionalized with fluoroalkyl siloxane chains[60] relative to those functionalized with alkyl siloxanes.

In order to interpret our data in terms of the variable under our control, the surface tension of the test liquids, γ_{LV}, and the variable that we measure (the apparent contact angle θ_{app}), we expressed Equations (3) and (4) in terms of surface tensions expressed in Equation (2).

$$\cos\theta_{app} = \frac{1}{\gamma_{LV}} r(\gamma_{SV} - \gamma_{SL}) \quad (5)$$

$$\gamma_{LV}\cos\theta_{app} = -f_2\gamma_{LV} + rf_1(\gamma_{SV} - \gamma_{SL}) \quad (6)$$

We plot $cos\ \theta_{app}$ versus $1/\gamma_{LV}$ for the various organosilanes on Whatman #1 paper (**Figure 3**a). Based on Equation (5), we expect our contact angle data to collapse to straight lines with zero intercepts, if the wetting of liquids followed the Wenzel model on silanized paper.

Figure 3a clearly demonstrates that the wetting behavior of liquids on silanized paper deviates significantly from the Wenzel model. When $\gamma_{LV}\ cos\ \theta_{app}$ was plotted versus γ_{LV}, we find that our data for silanized Whatman #1 paper collapses onto straight lines with negative slopes (Figure 3b), a behavior qualitatively consistent with Equation (6). The data for all the organosilanes tested fall within straight lines with slopes of -1 and -0.95 (i.e. $f_2 \sim$ between 1 and 0.95). This behavior suggests that the surface of the droplets primarily contacts the air pockets trapped at the interface with the paper surface. Similar behavior was observed for Whatman # 50 and Blot papers (data not shown).

To illustrate the effect of topography on the wettability of the papers, Figure 3c,d shows contact angle data plotted for two types of silanization (C_1^H and C_{10}^F) on the three different types of paper. Within the range of topographies we tested, liquids behave in a manner that is consistent with the Cassie-Baxter model. There is a clear and systematic deviation from the

linear trend of the contact angle data as the surface tension of the test liquids approached the wicking transition of the silanized papers. The deviation is present for all organosilane chemistries and for all types of paper tested (Figure 3c,d). We speculate that this deviation close to the wicking transition suggests a mode of wetting different from the classical Cassie-Baxter, and would be an interesting phenomenon to investigate.

3.5. R^F paper is superior to R^H paper for applications requiring minimal interactions with biological fluids

The wetting of silanized paper by biological fluids is important for its use in applications such as bioanalysis, cell culture, and drug discovery and development. Viscous solutions with a high content of protein or DNA, such as artificial saliva, a 5% (mass-to-mass ratio) solution of bovine serum albumin (BSA) in PBS, and a 500 μM solution of DNA in Tris-EDTA (TE) buffer, formed higher contact angles on fluorinated than on non-fluorinated papers of corresponding roughness (**Figure 4**c-f). In all cases, the longer the fluorinated alkyl chains, the higher the static contact angle.

Whole blood (fresh whole human blood, treated with an anticoagulant-preservative solution containing sodium heparin) and plasma formed contact angles larger than 150° on both R^H and R^F papers. Droplets of whole blood and plasma exhibit the lowest contact angle hysteresis (<15°) with fluorinated surfaces (Figure 4a-b). A drop of whole blood rolling on the surface of a strip of paper functionalized with C_{10}^F, and C_{12}^F did not leave a visible trace behind (**Figure 5**). The lack of staining is reminiscent of the behavior of the “slippery” omniphobic surfaces fabricated by the Aizenberg group,[47] and suggests a low level of cell and protein adhesion on the R^F paper.

For applications involving blood, it might be important to minimize the amount of trace liquid left behind on the surface (i.e. the surface should be self-cleaning). To test the performance of silanized paper, we deposited 50 μL drops of blood on the surface of various silanized papers that were initially horizontal. We then increased the tilt angle until the drop of blood rolled off the surface of the paper. **Figure 6**a shows representative images of the paper surfaces after the blood had rolled off. There are significantly more traces of blood left on the R^H papers than on the R^F papers. Papers treated with the organosilanes with the longer fluoroalkyl chains (C_{10}^F and C_{12}^F) showed no detectable trace of blood on the surface after roll-off. Figure 6b shows the roll-off angles measured for these papers. R^H papers had significantly higher roll-off angles than R^F papers. The blood drops adhered so strongly to C_{10}^H treated surfaces that the droplets did not fall off even when the paper was turned upside down (i.e. roll-off angle > 180^o). The state characterized by high adhesion and high contact angles has been termed the "petal effect"[64] and is attributed to hierarchical roughness (multiple length-scales of features) on surfaces.

3.6. Products formed on incineration of R^F paper

Bioanalytical devices fabricated using silanized paper can be disposed of by incineration; we wished to estimate the environmental impact of burning R^F paper. The elemental analysis of the fluorinated papers, suggests that the incineration of a 1 cm^2 device at T < 1500 °C can produce at most 34 μg of a perfluoroalkyl carboxylic acid; under more stringent conditions (temperatures above 1500 °C), this content of fluorine could lead to the formation of a maximum of ca. 29 μg of HF, or a maximum of ca. 49 μg of COF_2.

3.7. R^F paper is compatible with buffers commonly used in bioassays

We surveyed the wettability of silanized paper by common buffers, since the surface tension of an aqueous buffer can be dramatically altered by the addition of surfactants or other solutes. The buffers we surveyed include PBS, Tris, 1x Taq Buffer (used for polymerase chain reactions), Tris-Gly buffer (typically used in capillary electrophoresis); Lysogeny broth (LB) or Dulbecco's Modified Eagle Medium (DMEM)— buffers typically used for mammalian or bacterial cell culture. Buffers containing amines, amino acids, or dissolved salts form contact angles that are indistinguishable from that formed by pure water (Supporting Information, Figure S4).

An important distinction between the R^F and R^H surfaces however, is in their ability to resist wetting by aqueous solutions of nonionic surfactants. These surfactants reduce the surface tension of pure water to ~ 30 mN/m when present at or above the critical micelle concentration (cmc).[65] Nonionic surfactants are present in standard buffers used for PCR reactions, such as the 1x Taq Buffer. When used above the cmc, nonionic surfactants containing polyethylene oxide chains, (e.g. IGEPAL CA@630, Triton X-100 and Tween 20), wetted R^H, but not the R^F paper surfaces (Supporting Information, Figure S5). Therefore, R^H papers are not compatible with applications that require buffers containing nonionic surfactants.

3.8. Fabrication of functional three-dimensional omniphobic structures by simple creasing and folding of R^F paper

Gas-phase silanization does not affect the mechanical properties of the paper substrate. Thus, three-dimensional functional structures can be built by creasing or folding the paper, either

before or after silanization. We took advantage of the mechanical flexibility and foldability of the R^F paper to create microtiter plates from single sheets of paper using the principles of origami.[42] Two different designs were used for fabricating the microtiter plates: a square array of re-entrant honeycomb cells (**Figure 7**a), and a negative Poisson ratio structure based on a triangular array of re-entrant honeycomb cells[66] (Figure 7c). Figure 7 shows microtiter plates made from R^F paper holding an aqueous solution (DMEM, Figure 7b) and an organic liquid (toluene dyed with Sudan I, Figure 7d). The R^F paper structures formed stable walls that contained both liquids for a period of 14 days (which is simply the duration of our observation of the system). Under our experimental conditions, we did not observe a difference in the stability of structures fabricated by folding paper either before or after silanization (data not shown).

3.9. R^F paper infused with a perfluorinated liquid forms an omniphobic "SLIPS" surface exhibiting very low contact angle hysteresis

We introduced perfluoropolyether lubricant (Dupont™ Krytox® GPL 105) onto R^F paper surfaces. The liquid spontaneously spreads onto the whole substrate through capillary wicking, and the large pores in paper facilitate the infiltration and retention of the lubricating perfluoropolyether to form a continuous overlying film. **Figure 8** shows how R^F paper can serve as a substrate for SLIPS—"Slippery Liquid-infused Porous Substrates" with remarkably low hysteresis towards most liquids.[47, 67] Blood, toluene, and diethyl ether all slide off the paper SLIPS when the surface is tilted.

Figure 9a demonstrates that paper SLIPS show omniphobic behavior, with contact-angle hysteresis of the surface below 10° for all liquids we tested, and below 5° for most of

them. Paper SLIPS are also able to resist wetting by pentane, which has a surface tension of ~15 mN/m. Since the wetting characteristics (apparent contact angles θ_{app}, and hysteresis, $\theta_a - \theta_r$) of the paper SLIPS did not vary for the three types of paper substrates, we hypothesized that the film of perfluoropolyether oil dominates the wetting characteristics of this material.

To test this hypothesis, we measured the surface tension of the perfluoropolyether oil and the liquid-liquid interfacial tension between the perfluoropolyether oil and the test liquids using the pendant drop method. These values, along with the liquid-air surface tensions, provide all three surface energy components for calculating the equilibrium contact angle, θ_Y of our test liquids resting on a hypothetical smooth—solid surface that consisted only of the perfluoropolyether oil. We plot $\cos\theta_Y$,calculated using Equation (2) versus the $\cos\theta_{app}$ in Figure 9b, and find that indeed these values are strongly correlated. Thus, the wetting behavior of paper SLIPS can be reasonably predicted from the interfacial tension of a liquid of interest with the lubricating oil with Young's equation.

A useful feature of paper SLIPS is their foldability, which can be exploited for low-cost fabrication of structures with desired functionalities. Complex 3-D "slippery" structures of paper SLIPS can be easily fabricated using techniques based on (for example) origami directly from paper SLIPS, or from R^F paper folded, then impregnated with a perfluoropolyether. To demonstrated their mechanical flexibility and foldability, we folded paper SLIPS to make V-pleats and form "slippery" channels that can be used to guide droplets of toluene and methanol (**Figure 10**a, and Supporting Information, Movie S1). We created a simple switch by combining tilting with a pre-designed folded geometrical path. When the structure is tilted towards the left, the liquid droplet moves along the left hand channel (Figure 10b), while when the structure is tilted to the right, the path the liquid droplet takes is changed

and the droplet moves along the right-hand channel (Figure 10c). Paper SLIPS thus differ from those prepared by Aizenberg *et al.* in the ease with which (originally) planar sheets can be transformed into structures with complex topographies by folding.

3.10. Colorimetric detection of volatile compounds using R^F paper devices

R^F paper is repellant to liquids with surface tensions greater than 28 mN/m; at the same time, it is highly permeable to gases and compounds in the vapor phase. We folded R^F paper to create small (4 cm^3) parallelipipedically-shaped chambers that we used for the colorimetric detection of hydrogen sulfide and volatile primary amines. We contained an aqueous solution of either $CuSO_4$ or picrylsulfonic acid in the chamber and sealed its top with a transparent gas-impermeable tape (Fellowes adhesive sheet, PET/EVA/LDPE). A vial containing a solution of hydrogen sulfide or butylamine was placed underneath each chamber for 20s (see **Figure 11**b), to expose the chambers to the vapors of hydrogen sulfide and butyl amine, respectively; this experiment allowed the volatile compound to pass through the bottom wall and react with the solution contained in the R^F paper chamber. The volatile H_2S reacted with $CuSO_4$ to form a brown precipitate (CuS, Figure 11e); *n*-butylamine reacted with picrylsulfonic acid to form the orange product n-butyl 2,4,6 trinitroaniline (Figure 11h).

4. Conclusions

We show that a rapid, one-step reaction with a fluoroalkyl trichlorosilane in the gas phase transforms cellulose paper into R^F paper, an omniphobic material that is not wetted (θ_{app}> 90°) by water and organic liquids with surface tension as low as 28 mN/m. Upon impregnation with a perfluoropolyether lubricant, R^F paper forms a slippery material (paper

SLIPS) capable of repelling liquids with surface tensions as low as 15 mN/m. From a fabrication standpoint, cellulose-based paper is commercially available in a variety of forms – with different roughness, porosity, density, thickness, and flexibility – all of which can be converted into omniphobic materials or SLIPS upon appropriate surface functionalization, or upon functionalization and addition of a lubricant, to meet the needs of specific applications.

The potential for low cost for fabrication of R^F paper enables its use in applications that require gas permeable, disposable liquid barrier membranes, with possible uses as toxic gas sensors, membranes for lung-assist devices or fuel cells. R^F paper is more cost effective (~\$0.8/m^2 for cost of materials compared to prices of ~\$1500/m^2 for Nafion® to ~ \$29/m^2 for Gore-Tex®), but also more repellent to water than materials based on ePTFE: the advancing contact angles of water on R^F paper ($\theta_a^{H_2O}$ >150°) are higher than, for example, the contact angles of water on Gore-Tex membranes ($\theta_a^{H_2O}$ = ~ 110°).[68] Unlike other fluoropolymer-based quasi-omniphobic materials, such as SLIPS[43, 47, 67, 69] or omniphobic synthetic textured solids,[43] R^F paper and paper SLIPS are mechanically flexible materials that can be rolled and folded into a range of complex 3D structures with high stiffness and light weight. These materials are, however, susceptible to damage by stretching, or cutting.

We believe that the ability to resist wetting by liquids with a wide variety of surface tensions, combined with mechanical flexibility, foldability, light weight, biocompatibility (e.g. lack of wetting by blood), and gas permeability, make R^F paper a valuable new material, and a possible alternative to polymer-, glass-, and silicone- based materials now used as substrates for biomedical and bioanalytical applications, microfluidics, and MEMS.

Supporting Information

Supporting Information is available from the Wiley Online Library or from the author (http://gmwgroup.harvard.edu/pubs/index.php?b=2010&t=2019).

Acknowledgements

This work was supported by the Bill and Melinda Gates Foundation under award 51308.Work focusing on microtiter plates was supported by the Department of Energy (ER45852). R.V.M. acknowledges funding by the FP7 People program under the project Marie Curie IOF-275148. We thank Dr. Claudiu Stan and Dr. Barbara Smith for helpful discussions.

Received: ((will be filled in by the editorial staff))
Revised: ((will be filled in by the editorial staff))
Published online: ((will be filled in by the editorial staff))

References

1. F. Liu, B. Yi, D. Xing, J. Yu, H. Zhang, *J. Membr. Sci.* **2003**, *212*, 213.

2. H. Kajiwara, T. Hamada, Y. Ichikawa, M. Ishi, I. Yamazaki, *Artif. Organs* **2004**, *28*, 840.

3. H. K. Inoue, S. Kobayashi, K. Ohbayashi, H. Kohga, M. Nakamura, *J. Neurosurg.* **1994**, *80*, 689.

4. C. Minale, G. Hollweg, S. Nikol, C. Mittermayer, B. J. Messmer, *Thorac. Cardiovasc. Surg.* **1987**, *35*, 312.

5. R. Bardini, V. Radicchi, P. Parimbelli, S. M. Tosato, S. Narne, *Ann. Thorac. Surg.* **2003**, *76*, 304.

6. R. Sreenivasan, E. K. Bassett, D. M. Hoganson, J. P. Vacanti, K. K. Gleason, *Biomaterials* **2011**, *32*, 3883.

7. K. Esato, B. Eiseman, *J. Thorac. Cardiovasc. Surg.* **1975**, *69*, 690.

8. X. Liu, M. Mwangi, X. Li, M. O'Brien, G. M. Whitesides, *Lab Chip* **2011**, *11*, 2189.

9. E. Carrilho, A. W. Martinez, G. M. Whitesides, *Anal. Chem.* **2009**, *81*, 7091.

10. A. W. Martinez, S. T. Phillips, G. M. Whitesides, E. Carrilho, *Anal. Chem.* **2010**, *82*, 3.

11. J. M. Zhang, J. Zhang, *Acta. Polym. Sin.* **2010**, 1376.

12. R. Martins, I. Ferreira, E. Fortunato, *Phys. Status Solidi RRL* **2011**, *5*, 332.

13. E. Fortunato *et al.*, *IEEE Electr. Device L.* **2008**, *29*, 988.

14. S. Yun, S.-D. Jang, G.-Y. Yun, J.-H. Kim, J. Kim, *Appl. Phys. Lett.* **2009**, *95*.

15. J. Kim, S. H. Bae, H. G. Lim, *Smart Mater. Struct.* **2006**, *15*, 889.

16. S. K. Mahadeva, S. Yun, J. Kim, *J. Intel. Mat. Syst. Str.* **2009**, *20*, 1141.

17. K. M. Suresha, S. Y. Yang, M. H. Lee, J.-H. Kim, J. Kim, *Compos. Interface.* **2008**, *15*, 679.

18. A. D. Mazzeo *et al.*, *Adv. Mater.* **2012**, *24*, 2850.

19. A. C. Siegel, S. T. Phillips, B. J. Wiley, G. M. Whitesides, *Lab Chip* **2009**, *9*, 2775.

20. R. Derda *et al.*, *PLoS One* **2011**, *6*, e18940.

21. A. W. Martinez, S. T. Phillips, B. J. Wiley, M. Gupta, G. M. Whitesides, *Lab Chip* **2008**, *8*, 2146.

22. E. Malmstrom, A. Carlmark, *Polym. Chem.* **2012**, *3*, 1702.

23. S. Kalia *et al.*, *Int. J. Polym. Sci.* **2011**, Article ID 837875.

24. A. G. Cunha, A. Gandini, *Cellulose* **2010**, *17*, 875.

25. C. S. R. Freire, A. Gandini, *Cellul. Chem. Technol.* **2006**, *40*, 691.

26. H. A. Schuyten, J. D. Reid, J. W. Weaver, J. G. Frick, *Text. Res. J.* **1948**, *18*, 396.

27. J. Shen, X. R. Qian, *Bioresources* **2012**, *7*, 4495.

28. Z. Guo, W. Liu, B. L. Su, *J. Colloid Interf. Sci.* **2011**, *353*, 335.

29. H. Ogihara, J. Xie, J. Okagaki, T. Saji, *Langmuir* **2012**, *28*, 4605.

30. K. Abe, K. Suzuki, D. Citterio, *Anal. Chem.* **2008**, *80*, 6928.

31. B. Balu, V. Breedveld, D. W. Hess, *Langmuir* **2008**, *24*, 4785.

32. Q. He, C. Ma, X. Hu, H. Chen, *Anal. Chem.* **2012**.

33. H. S. Khoo, F. G. Tseng, *Nanotechnology* **2008**, *19*.

34. M. J. Oh, S. Y. Lee, K. H. Paik, *J. Ind. Eng. Chem.* **2011**, *17*, 149.

35. A. Cunha, A. Gandini, *Cellulose* **2010**, *17*, 875.

36. C. Gaiolas, A. P. Costa, M. Nunes, M. J. S. Silva, M. N. Belgacem, *Plasma Process. Polym.* **2008**, *5*, 444.

37. G. R. J. Artus, S. Seeger, *Ind. Eng. Chem. Res.* **2012**, *51*, 2631.

38. J. Zimmermann, F. A. Reifler, G. Fortunato, L.-C. Gerhardt, S. Seeger, *Adv. Funct. Mater.* **2008**, *18*, 3662.

39. M. A. Shirgholami, M. S. Khalil-Abad, R. Khajavi, M. E. Yazdanshenas, *J. Colloid Interf. Sci.* **2011**, *359*, 530.

40. F. J. Norton, *Production of water-repellent materials*, United States Patent Office, 427/255.393 **1943**, United States Patent Office, 427/255.393.

41. D. Nystrom, J. Lindqvist, E. Ostmark, A. Hult, E. Malmstrom, *Chem. Commun.* **2006**, 3594.

42. P. Jackson, *Folding Techniques for Designers. From Sheet to Form*, Laurence King Publishing Ltd, London, U.K. **2011**.

43. A. Tuteja, W. Choi, J. M. Mabry, G. H. McKinley, R. E. Cohen, *Proc. Natl. Acad. Sci. U. S. A.* **2008**, *105*, 18200.

44. Z. G. Guo, W. M. Liu, B. L. Su, *J. Colloid Interf. Sci.* **2011**, *353*, 335.

45. E. Wang *et al.*, *Microfluid. Nanofluid.* **2009**, *7*, 137.

46. A. Sidorenko, T. Krupenkin, J. Aizenberg, *J. Mater. Chem.* **2008**, *18*, 3841.

47. T. S. Wong *et al.*, *Nature* **2011**, *477*, 443.

48. A. Voller, D. E. Bidwell, A. Bartlett, *Bull. World Health Organ.* **1976**, *53*, 55.

49. C. D. Chin *et al.*, *Nat. Med.* **2011**, *17*, 1015.

50. C. M. Cheng *et al.*, *Angew. Chem.* **2010**, *49*, 4771.

51. E. Verpoorte, *Electrophoresis* **2002**, *23*, 677.

52. E. M. Southern, *J. Mol. Biol.* **1975**, *98*, 503.

53. M. A. Burns *et al.*, *Science* **1998**, *282*, 484.

54. K. A. Mirica, S. T. Phillips, C. R. Mace, G. M. Whitesides, *J. Agric. Food Chem.* **2010**, *58*, 6565.

55. R. S. Lanciotti, C. H. Calisher, D. J. Gubler, G. J. Chang, A. V. Vorndam, *J. Clin. Microbiol.* **1992**, *30*, 545.

56. P. Yager *et al.*, *Nature* **2006**, *442*, 412.

57. I. Meyvantsson, D. J. Beebe, in *Annu. Rev. Anal. Chem.* (2008), vol. 1, pp. 423.

58. G. Kohler, C. Milstein, *Nature* **1975**, *256*, 495.

59. J. Monod, *Annu. Rev. Microbiol.* **1949**, *3*, 371.

60. A. W. Adamson, A. P. U. Gast, *Physical Chemistry of Surfaces*, Wiley, **1997**, 368.

61. G. R. J. Artus *et al.*, *Adv. Mater.* **2006**, *18*, 2758.

62. P. G. De Gennes, F. Brochard-Wyart, D. Quere, *Capillarity and wetting phenomena: drops, bubbles, pearls, waves*, Springer, **2003**.

63. G. L. E. Turner, *CRC Handbook of Chemistry and Physics, 70th Ed.* Vol. 48, **1991**.

64. L. Feng *et al.*, *Langmuir* **2008**, *24*, 4114.

65. M. J. Rosen, *Surfactants and Interfacial Phenomena*, John Wiley & Sons, Holboken **2004**.

66. R. Lakes, *Adv. Mater.* **1993**, *5*, 293.

67. A. K. Epstein, T. S. Wong, R. A. Belisle, E. M. Boggs, J. Aizenberg, *Proc. Natl. Acad. Sci. U. S. A.* **2012**, *109*, 13182.

68. M. Rzechowicz, R. M. Pashley, *J. Colloid Interf. Sci.* **2006**, *298*, 321.

69. P. Kim *et al.*, *ACS Nano* **2012**, *6*, 6569.

Figure 1

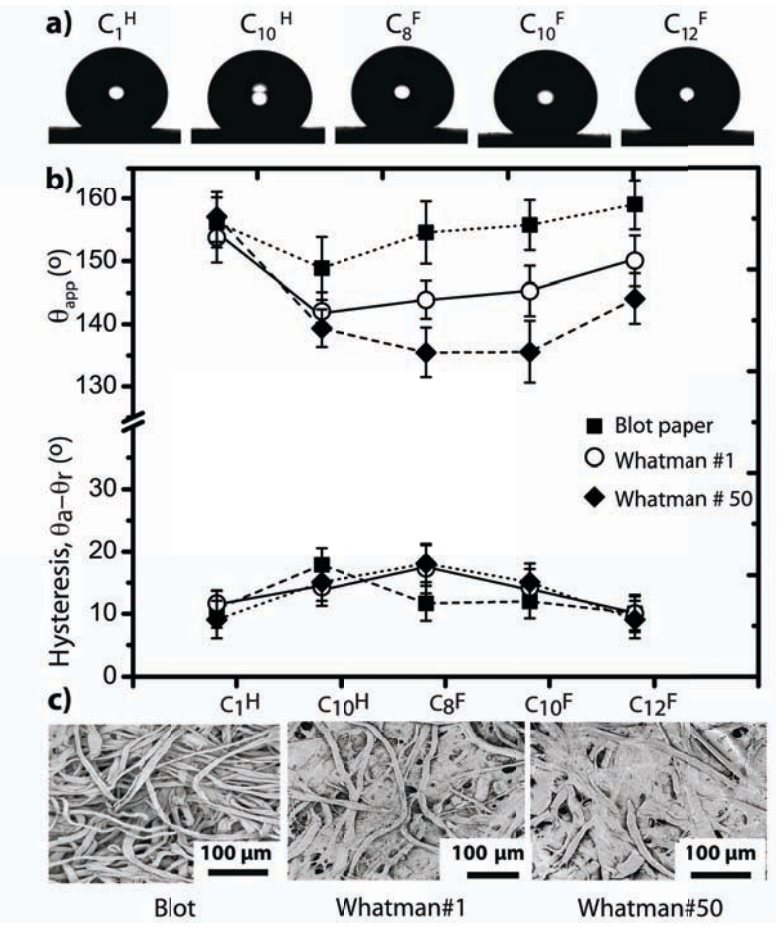

Figure 1. a) Representative images of water droplets on silanized paper. b) Static contact angles θ_{app}, and contact angle hysteresis $(\theta_a-\theta_r)$ of water on silanized paper for three types of paper with different surface functionalization. Hollow symbols represent angles with Gel Blot paper (Blot), grey filled symbols represent angles with Whatman#1 paper (W1), and black filled symbols represent angles with Whatman #50 paper (W50). The volume of each drop is 10 µL. Error bars: standard deviations for N=30 measurements. c) SEM images showing the topography of the different paper surfaces.

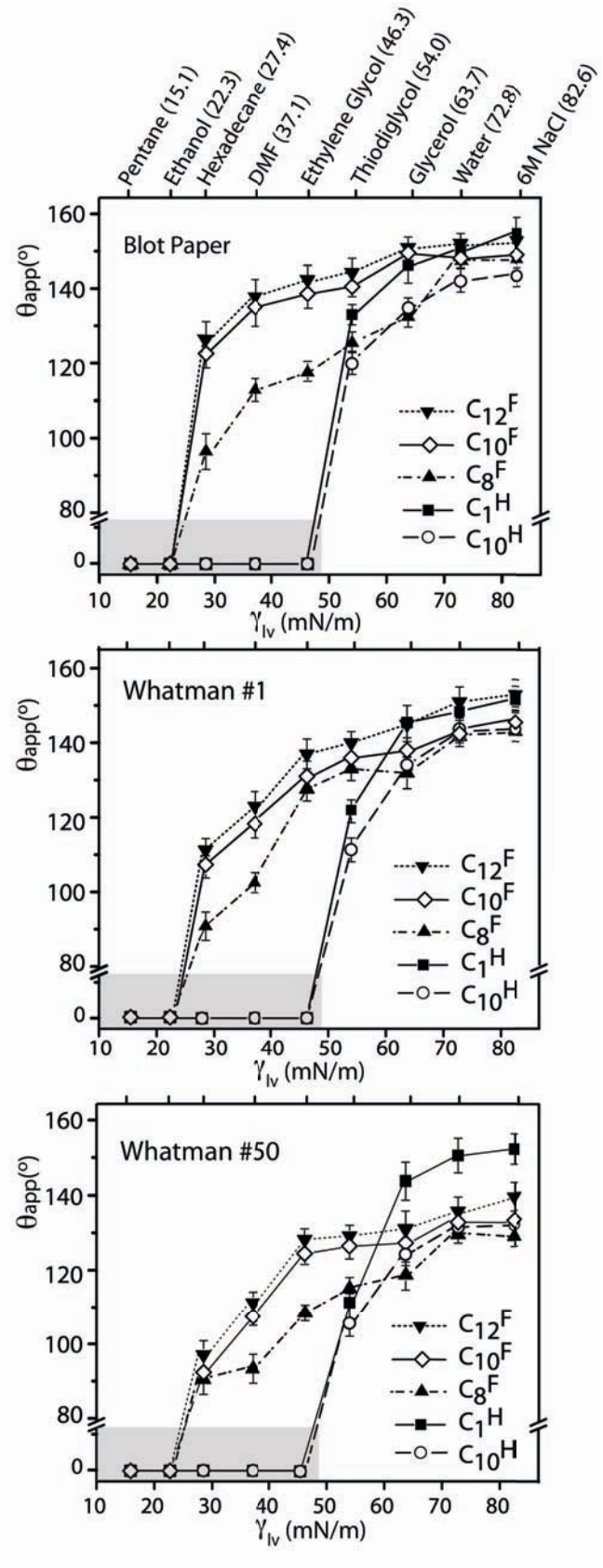
Pentane (15.1)
Ethanol (22.3)
Hexadecane (27.4)
DMF (37.1)
Ethylene Glycol (46.3)
Thiodiglycol (54.0)
Glycerol (63.7)
Water (72.8)
6M NaCl (82.6)
Blot Paper
Whatman #1
Whatman #50
θapp(°)
γlv (mN/m)
C12F
C10F
C8F
C1H
C10H

Figure 2: The dependence of static contact angles on surface tension for 10 µL droplets of liquid. The liquids used in these experiments and their respective surface tensions (γ_{LV}) at 20°C in mN/m are (literature values [63]): pentane (15.5), anhydrous ethanol (22.3), hexadecane (27.4), DMF (37.1), ethylene glycol (46.3), thiodiglycol (54.0), glycerol (63.7), water (72.8), 6m NaCl (82.6). Error bars: standard deviation for N=30 measurements. The grey area indicates liquids that spontaneously spread onto the substrate through capillary wicking.

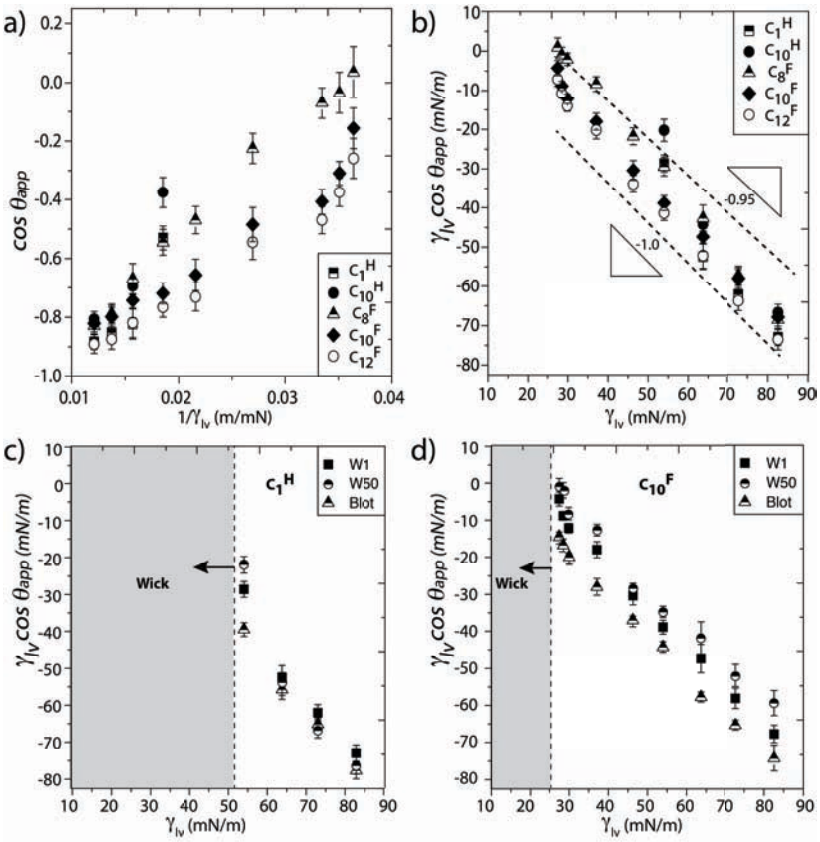

Figure 3: Analysis of liquid contact angle data on silanized paper. a) Plot of $cos\ \theta_{app}$ versus $1/\gamma_{LV}$ for the five silanes of differing chain lengths and degree of fluorination on Whatman #1 paper. b) Plot of $\gamma_{LV}\ cos\ \theta_{app}$ versus γ_{LV} for the five silanes of differing chain lengths and degree of fluorination on Whatman#1 paper. The data collapses onto straight lines, indicative of Cassie-Baxter type wetting, with slopes in the range of -1.0 and -0.95. These values indicate that a large area fraction of the droplets is resting on air. c) Plot of $\gamma_{LV}\ cos\ \theta_{app}$ versus γ_{LV} for three different types of paper, each treated indistinguishably with C_1^H silane. d) Plot of $\gamma_{LV}\ cos\ \theta_{app}$ versus γ_{LV} for three different types of paper each treated indistinguishably with C_{10}^F silane. For the three types of paper we analyzed, topography appears to have a smaller effect on liquid repellency than the degree of fluorination of the organosilane.

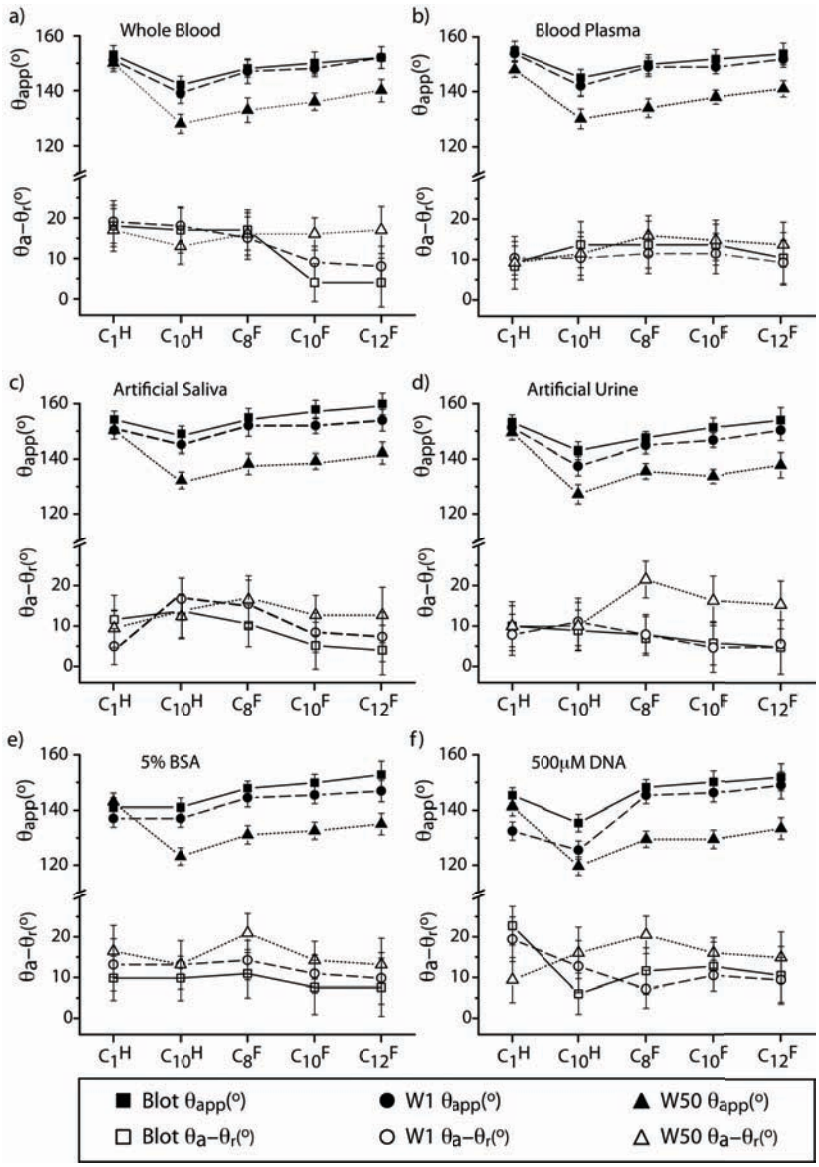

Figure 4: Static contact angles (filled symbols) and hysteresis *(θ_a-θ_r)* (hollow symbols) of several biological fluids: a) whole blood, b) plasma, c) artificial saliva, d) artificial urine, e) a solution of protein (5% BSA in PBS), and f) a solution of DNA (500μM of DNA in TE buffer) on functionalized Gel Blot (square symbols), Whatman #1 (circular symbols) and Whatman #50 (triangular symbols). Error bars: standard deviation for N=30 measurements.

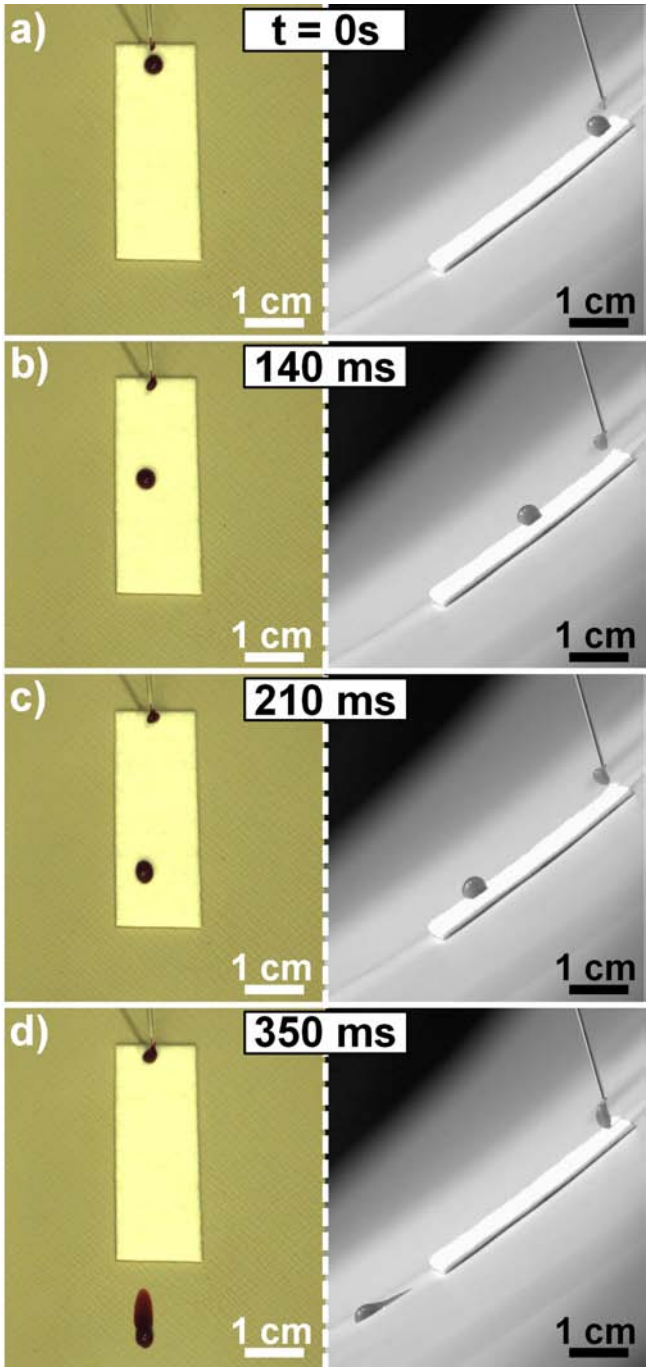

Figure 5: Time-sequence images of a drop of heparinized human blood rolling down on Gel Blot paper functionalized with C_{10}^{F} (side view: left; front view: right). The rolling drop does not leave a stain visible to the unaided eye.

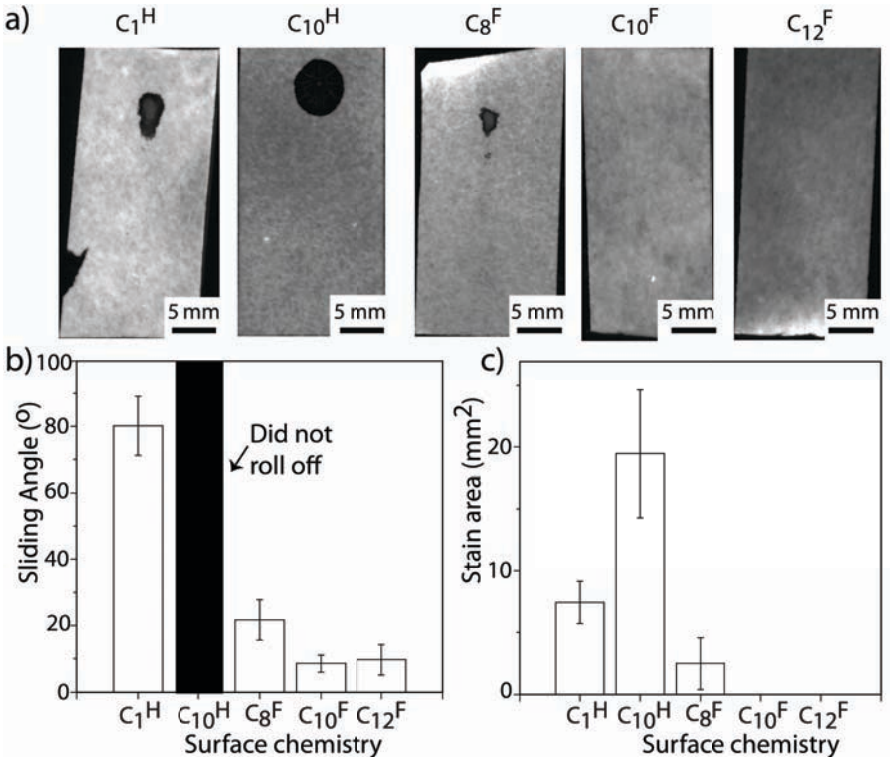

Figure 6: a) Images obtained with a fluorescence gel scanner from silanized paper after the drop of blood released and rolled off on tilted paper. The dark spots are dried blood. b) The angles of incline at which the droplets of blood rolled off the silanized papers. c) The amount of blood adhering to the paper after the blood droplet had rolled off, quantified as the area of the blood stain left on the paper. Bars are standard deviations for N=7 measurements.

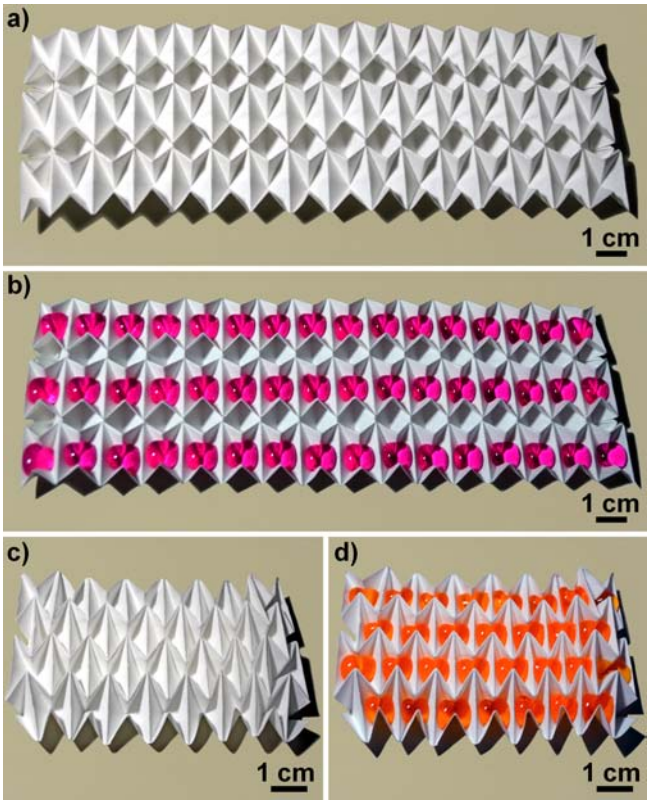

Figure 7: Omniphobic microtiter plates fabricated by creasing and folding of R^F paper: a) a square array of re-entrant honeycomb cells, and c) a negative Poisson ratio structure based on a triangular array of re-entrant honeycomb cells. These structures are able to stably hold in each well 500 µL of b) aqueous solutions (Dulbecco's Modified Eagle Medium) and d) organic liquids (toluene dyed with Sudan I).

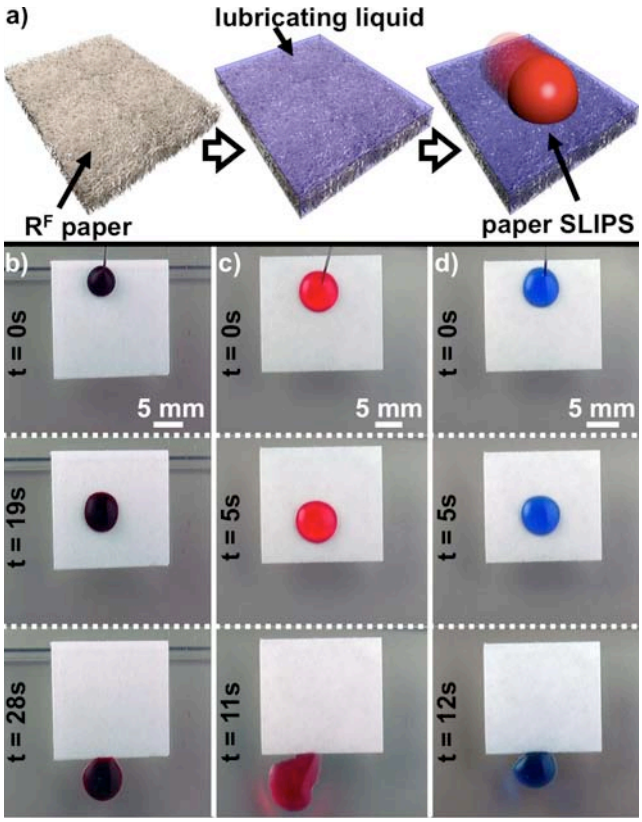

Figure 8: a) Fabrication of paper slippery porous liquid-infused surfaces (paper SLIPS) from R^F paper impregnated with a perfluoropolyether. Time-sequence images showing rolling droplets of: b) heparinized human blood (volume ~30 µL), c-d) diethyl ether dyed with Sudan Red (γ_{LV}=17 mN/m, volume ~30 µL) and h-j) toluene dyed with Sudan Blue (γ_{LV} = 28 mN/m, volume ~30 µL) on a paper SLIPS at ~5° tilting.

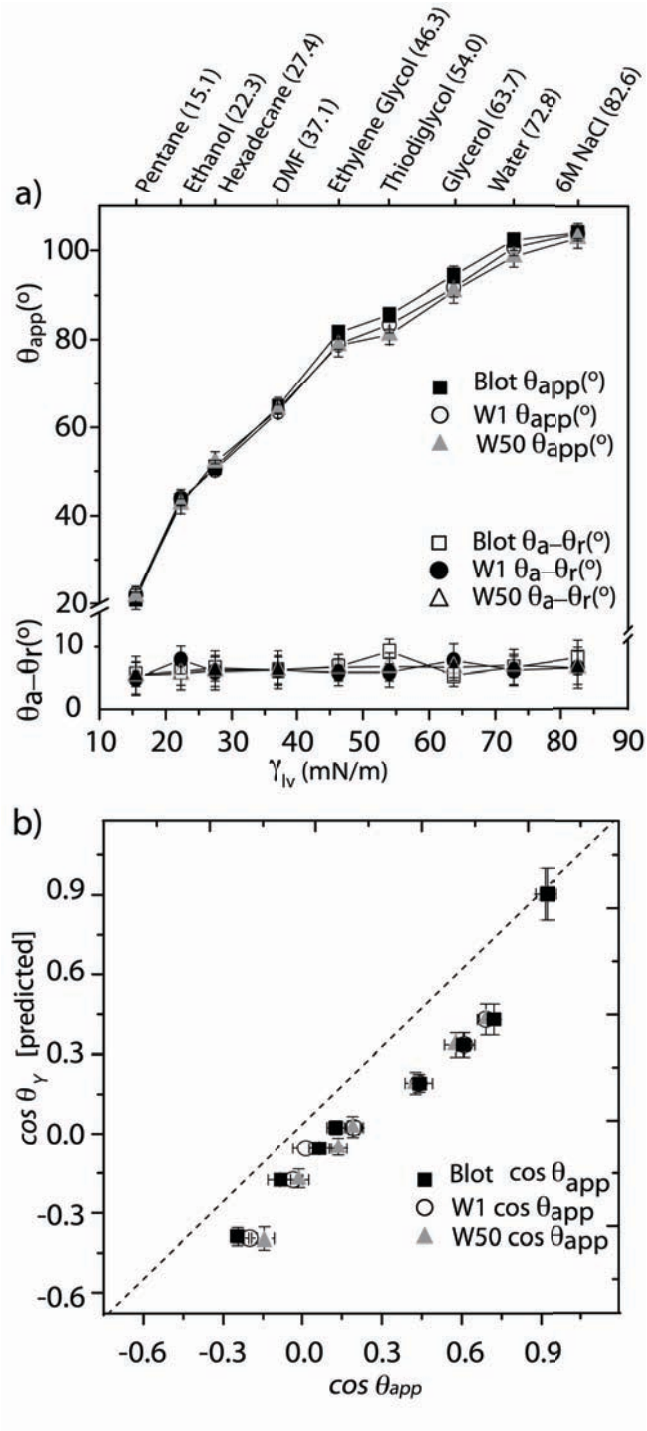

Figure 9: a) Comparison of apparent contact angles and contact angle hysteresis (θ_a-θ_r) as a function of surface tension of test liquids (indicated) for SLIPS fabricated from Gel Blot, Whatman #1 and Whatman #50 paper silanized with C_{10}^F and impregnated with a perfluoropolyether lubricant (Dupont™ Krytox® GPL 105). b) Plot of the cosine of the predicted equilibrium contact angle—calculated with the assumption that the liquids wet a

hypothetical flat surface composed solely of perfluoropolyether lubricant—versus the cosine of the measured apparent angle of liquids with the paper SLIPS. The diagonal dashed line is drawn to guide the eye to show the case of perfect correlation.

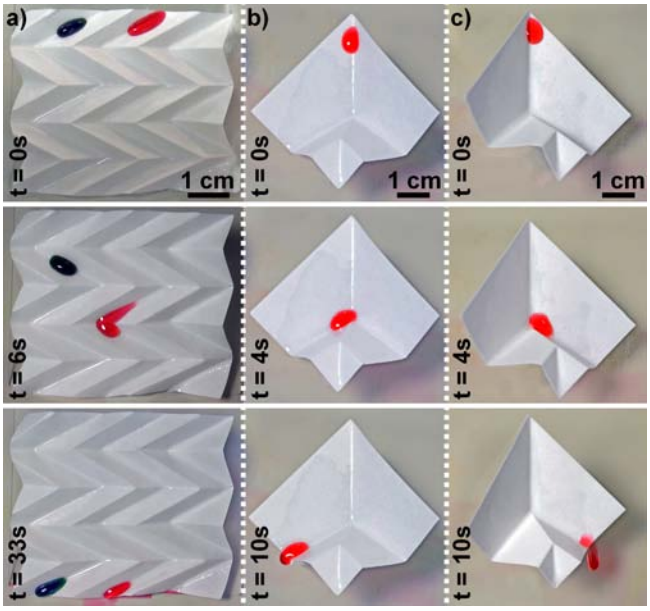

Figure 10: 3-D "slippery" structures fabricated by folding and creasing R^F paper impregnated with a perfluoropolyether lubricant (Krytox® GPL105). The paper was first impregnated, and then creased. These structures can guide the transport of liquid droplets of dyed methanol (green) and dyed toluene (red) using a) a slippery "channel" formed by successive V-pleats in a paper SLIPS or b-c) a fluidic switch formed by combining tilting and a pre-defined geometry.

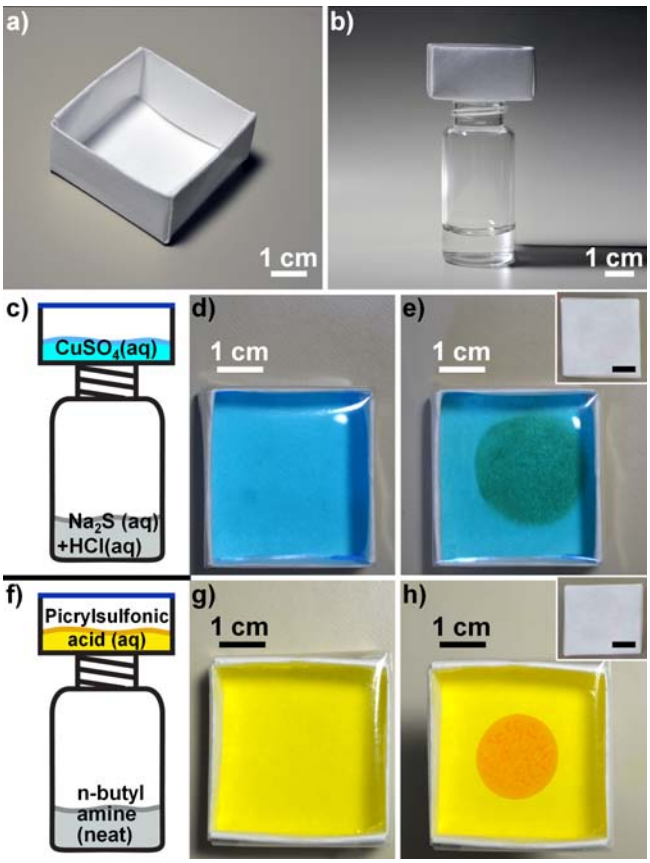

Figure 11: Gas permeable but liquid impermeable "chambers" fabricated by folding and creasing R^F paper and sealing the top with a gas-impermeable tape (Fellowes adhesive sheet, PET/EVA/LDPE) can be used as colorimetric sensors to detect either hydrogen sulfide or volatile primary amines. a) Design of the "chamber" and b) design of the experiment. Each sealed "chamber" contained an aqueous solution of either d) $CuSO_4$ or g) picrylsulfonic acid (1M in water). When the paper structure is exposed to a volatile source of H_2S or butyl amine, the solution in the "chamber" forms e) a brown precipitate (CuS), or h) an orange product (*n*-butyl-2,4,6-trinitroaniline). The insets depict the bottom of the chamber after the colorimetric detection occurred.

Table of Contents

Omniphobic "R^F" paper (paper that is both hydrophobic and oleophobic) is formed by silanization of the cellulose fibers of paper with fluoroalkyl chains. R^F paper is highly permeable to gases and mechanically flexible, which allows it to be folded into functional shapes to form microtiter plates and liquid-filled gas sensors.

Keywords: Omniphobic Paper, SLIPS, Paper SLIPS, Origami, Hydrophobic Paper.

Ana C. Glavan, Ramses V. Martinez, Anand Bala Subramaniam, Hyo Jae Yoon, Rui M.D. Nunes, Heiko Lange, Martin M. Thuo, and George M. Whitesides*

Omniphobic "R^F Paper" Produced by Silanization of Paper with Fluoroalkyltrichlorosilanes

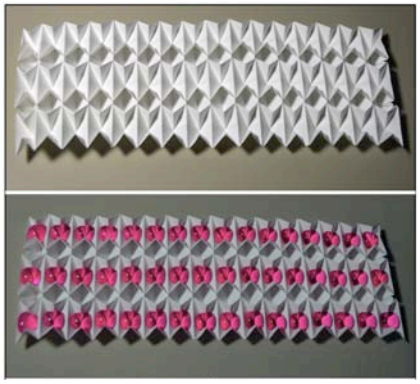

ADVANCED FUNCTIONAL MATERIALS

Supporting Information

for *Adv. Funct. Mater.*, DOI: 10.1002/adfm. XX.

Omniphobic "R^F Paper" Produced by Silanization of Paper with Fluoroalkyltrichlorosilanes

Ana C. Glavan, Ramses V. Martinez, Anand Bala Subramaniam, Hyo Jae Yoon, Rui M.D. Nunes, Heiko Lange, Martin M. Thuo, and George M. Whitesides

"Omniphobic "R^F Paper" Produced by Silanization with Fluoroalkyltrichlorosilanes"

By *Ana C. Glavan*[1], *Ramses V. Martinez*[1†], *Anand Bala Subramaniam*[1†], *Hyo Jae Yoon*[1], *Rui M.D. Nunes*[1], *Heiko Lange*[1], *Martin M. Thuo*[1], *and George M. Whitesides*[1,2*]

Supporting Information

Materials and Methods

Fabrication of R^H and R^F papers. The silanizing reagents: i) tricholoromethylsilane (CH_3SiCl_3, "C1H"), trichlorodecylsilane ($CH_3(CH_2)_9SiCl_3$, "$C_{10}{}^H$"), trichloro(3,3,4,4,5,5,6,6,7,7,8,8,8-tridecafluorooctyl)silane ($CF_3(CF_2)_5CH_2$-CH_2SiCl_3, "$C_8{}^F$"), trichloro(3,3,4,4,5,5,6,6,7,7,8,8,9,9,10,10,10-heptadecafluorodecyl)silane ($CF_3(CF_2)_7CH_2$-CH_2SiCl_3, "$C_{10}{}^F$"), trichloro (3,3,4,4,5,5,6,6,7,7,8,8,9,9,10,10, 11,11, 12,12,12-henicosafluorododecyl)silane ($CF_3(CF_2)_9CH_2$-CH_2SiCl_3, "$C_{12}{}^F$) were purchased from Gelest Inc (Morrisville, PA). All chemicals were used as received without further purification. Paper (Gel Blot paper, Whatman#1, and Whatman#50) was purchased from GE Healthcare (NJ, USA) and used as received, without purification.

The silanization reaction was conducted in a chamber with a volume of 0.01 m^3 at a temperature set at 95 °C. The silanizing reagent is transferred into a glass vial under inert gas atmosphere and placed inside the chamber together with the samples. Each experiment typically required approximately 100 mg of silane in 5 mL of anhydrous toluene. The silane

was vaporized at 95 °C under reduced pressure (~30 mbar, 0.03 atm) and allowed to react for 5 minutes. Diffusion inside the reaction chamber is sufficient for an even distribution of the silane within the chamber.

Characterization of the wettability of different papers. Solvents were used as received: Pentane (Sigma-Aldrich, anhydrous, ≥99%), diethyl ether (Sigma-Aldrich, anhydrous, ≥99%), perfluorodecalin (Sigma-Aldrich, anhydrous, ≥99%), anhydrous ethanol (Pharmco-Aaper, 200 proof, absolute), *n*-hexadecane (Sigma-Aldrich, anhydrous, ≥99%), DMF (Sigma-Aldrich, anhydrous, ≥99%), ethylene glycol (Sigma-Aldrich, anhydrous, ≥99%), thiodiglycol (Sigma-Aldrich, anhydrous, ≥99%), toluene (Acros, spectrophotometric grade 99+%), dimethylsulfoxide (DMSO, Sigma-Aldrich, anhydrous 99.9%), methanol (Ashland, VLSI). Human heparinized whole blood and human plasma were purchased from Research Blood Components, LLC (Brighton, MA). All surfactants were purchased from Sigma-Aldrich (St. Louis, MO). Water is ultrapure and deionized (resistivity > 18.2 MΩ cm).

Contact angle measurements. The contact angle measurements were performed using a contact angle measurement system (Ramé-Hart model 500-F1, Ramé-Hart Instrument Co.) at room temperature (20 – 25 °C) with ~20% relative humidity. The droplet volume for the measurement was ~10 μL (unless otherwise specified). The advancing and receding contact angles were measured by the sessile drop method, which involves expanding or contracting a contact angle droplet by adding or withdrawing fluid in 1 μL increments. The droplet profile was fitted to a spherical profile using the software provided by the system. The advancing contact angles are measured at the leading droplet edge when the value of the contact angle remained constant and solid/liquid interface started to increase; the receding angles were

measured at the trailing droplet edge when the value of the contact angle remained constant and the solid/liquid interface started to decrease.

Scanning electron imaging. Scanning electron microscope (SEM) images (Fig. 2 B, C inset) of the paper microfluidic device was acquired with a Zeiss Supra 55 VP FESEM at 2 kV at a working distance of 6 mm. Before SEM imaging, the sample was sputter coated with Pt/Pd at 60 mA for 15–45 s.

RMS Roughness measurements of paper. We measured the height RMS roughness with a Taylor-Hobson CCI HD Optical Profiler according to the ISO25178 norm. The CCI method is based on the cross-coherence analysis of two low-coherence light sources, the beam reflected from our sample and a reference beam reflected from a reference mirror. Paper has a low reflectance that hinders the application of interferometry techniques. To improve the reflectance of paper we deposited a conformal thin layer of Au (~4 nm) using a Cressington 208HR sputter coater. In each experiment, at least seven 0.4 μm x 0.4 μm areas were analyzed.

Preparation of SLIPS. Lubricating fluid (Dupont™ Krytox® GPL 105), was added to the surfaces (~50 μL/cm^2) by pipette to impregnate the paper and form a coating film. The fluid spontaneously spread onto the whole substrate through capillary wicking. Tilting the surface and mildly applying compressed air removed the excess of lubricating fluid.

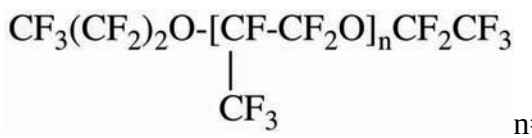

Dupont™ Krytox® GPL 105: molecular structure

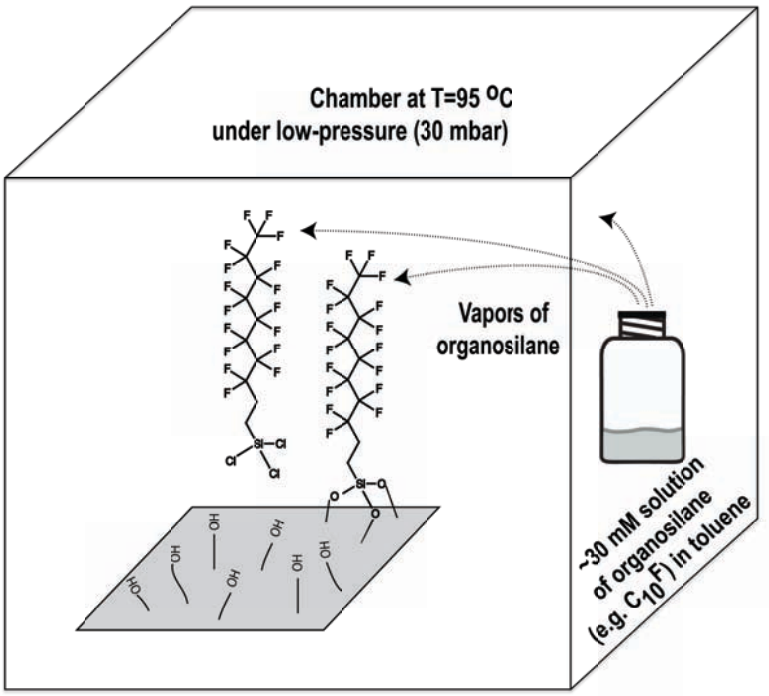

Figure S1: Schematic representation of the process used for surface modification of paper surfaces *via* silanization.

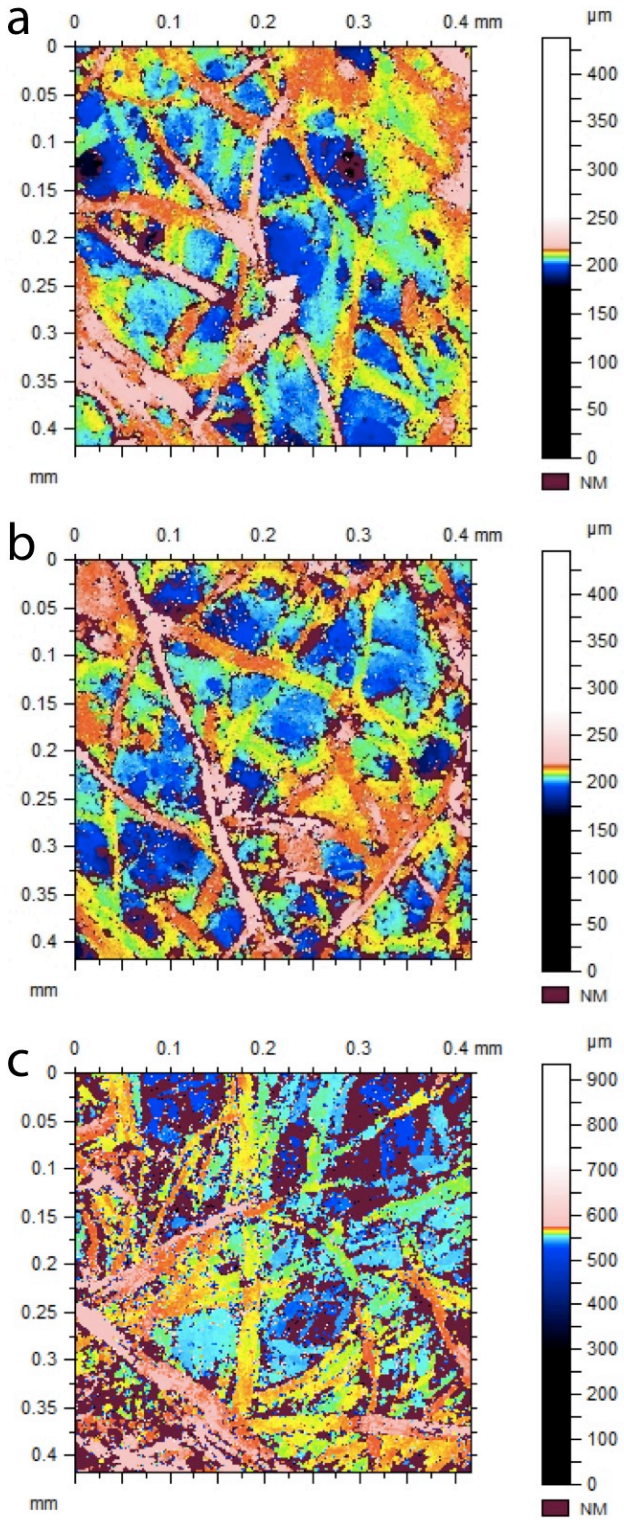

Figure S2: Optical profilometry images of Whatman #1 (W1), Whatman #50 (W50), Gel Blot paper (Blot)

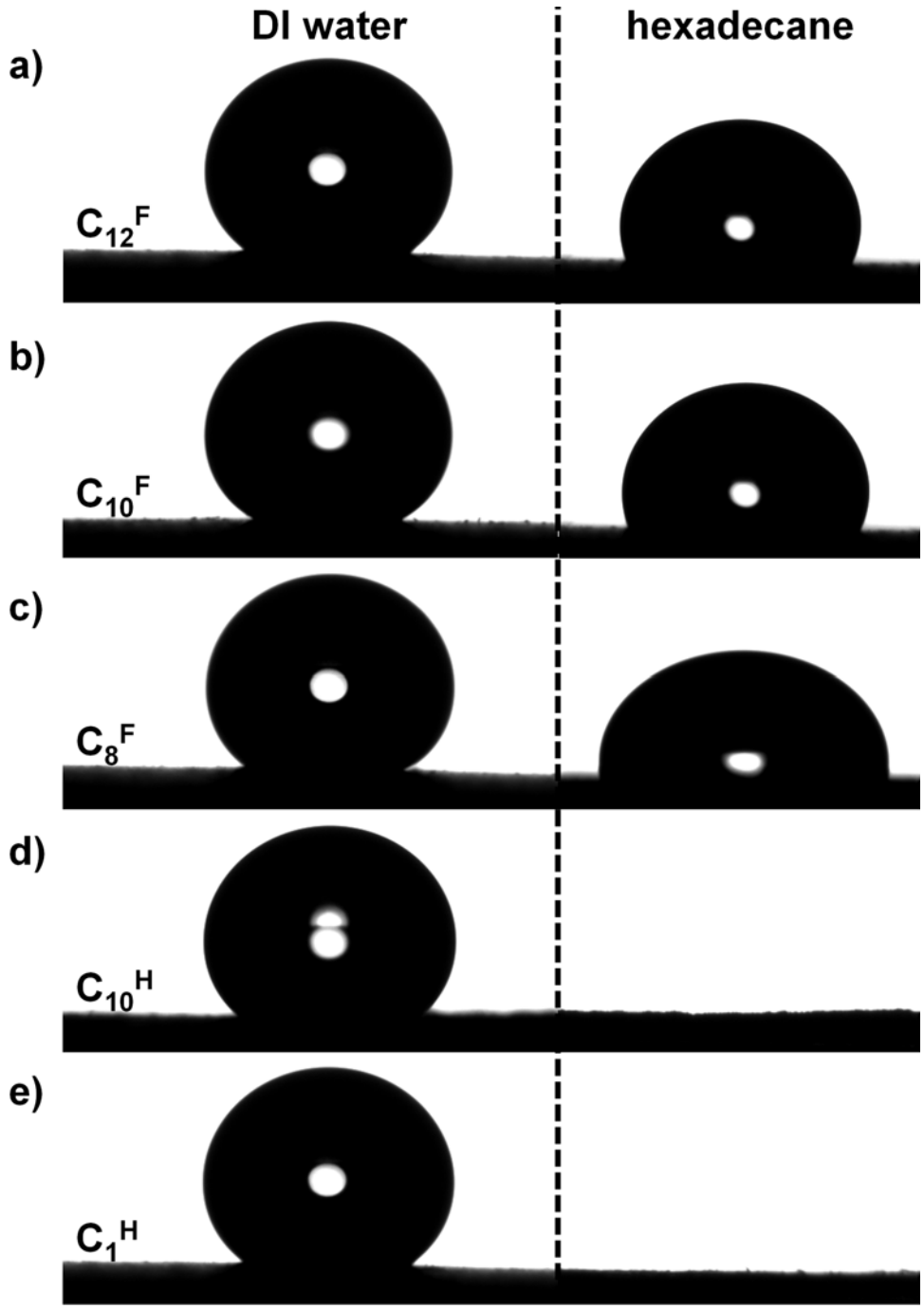

Figure S3: Droplets of water and hexadecane on Whatman #1 functionalized with alkyl and fluoroalkyl trichlorosilanes. The volume of each droplet is 10 μL.

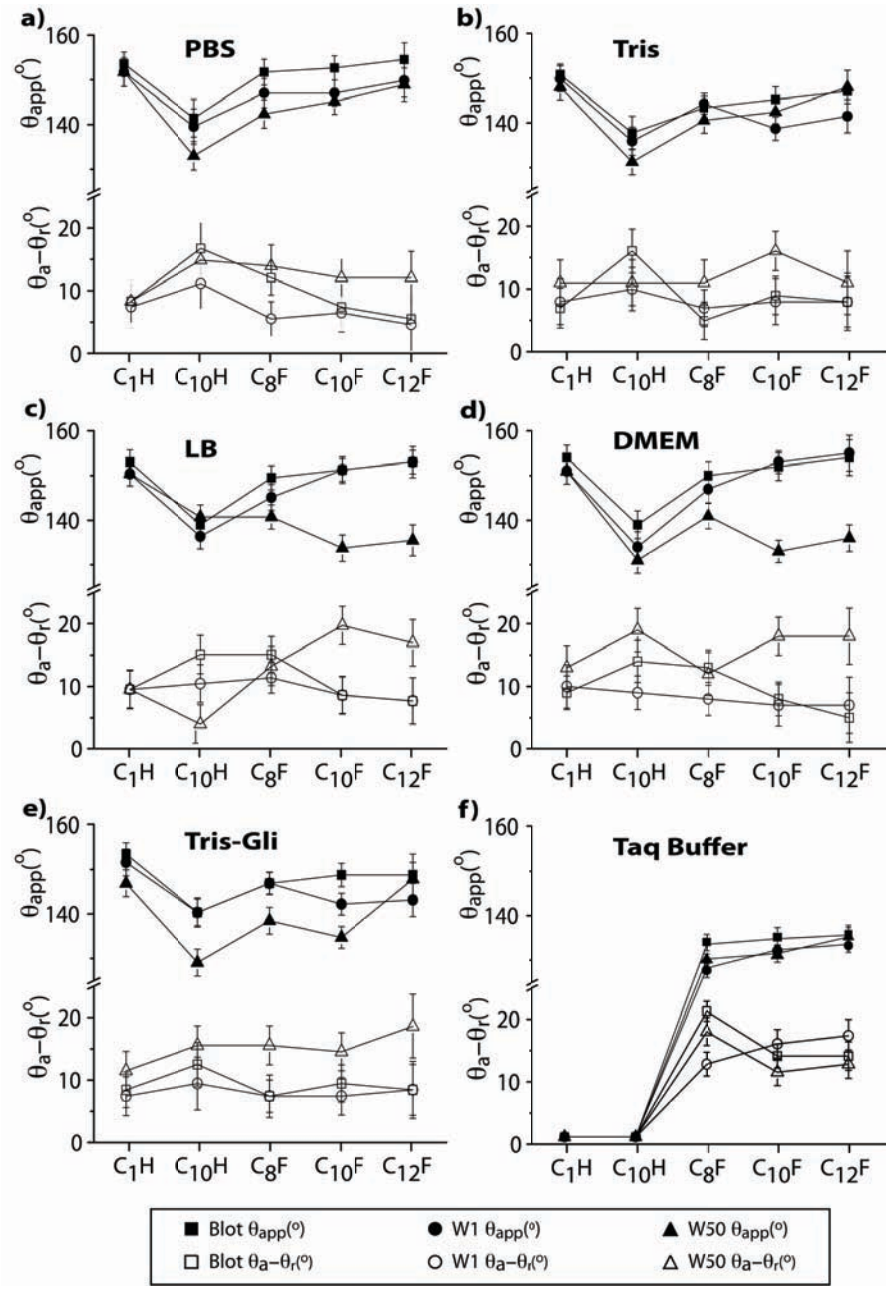

Figure S4: Static contact angles (filled symbols) and hysteresis (hollow symbols) for several buffers commonly used in biological applications: PBS (pH 7.2), Tris (pH 7.4), LB, DMEM, Tris-Gly Buffer (pH 8.3), and 1x OneTaq MasterMix (typical PCR buffer) on functionalized Gel Blot, Whatman #1 and Whatman #50 paper. The 1x OneTaq Mastermix is an aqueous solution that notably wets the non-fluorinated surfaces. Error bars represent standard deviation (N=30).

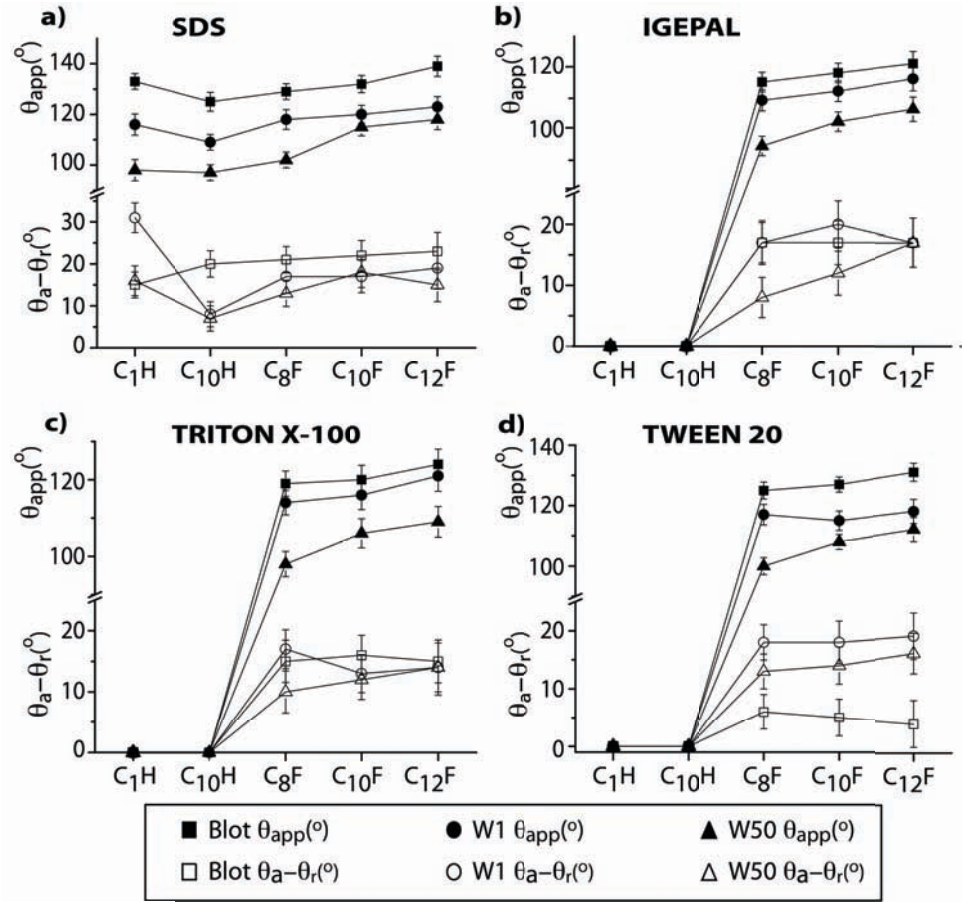

Figure S5: Static contact angles (filled symbols) and hysteresis (hollow symbols) of aqueous solutions of detergent commonly used in molecular biology on functionalized Blotting, Whatman#1 and Whatman#50 paper. The non-fluorinated surfaces are wetted by 0.05% TritonX, 0.07% Tween 20 and 0.05% IGEPAL@CA630. Error bars represent standard deviation (N=30).

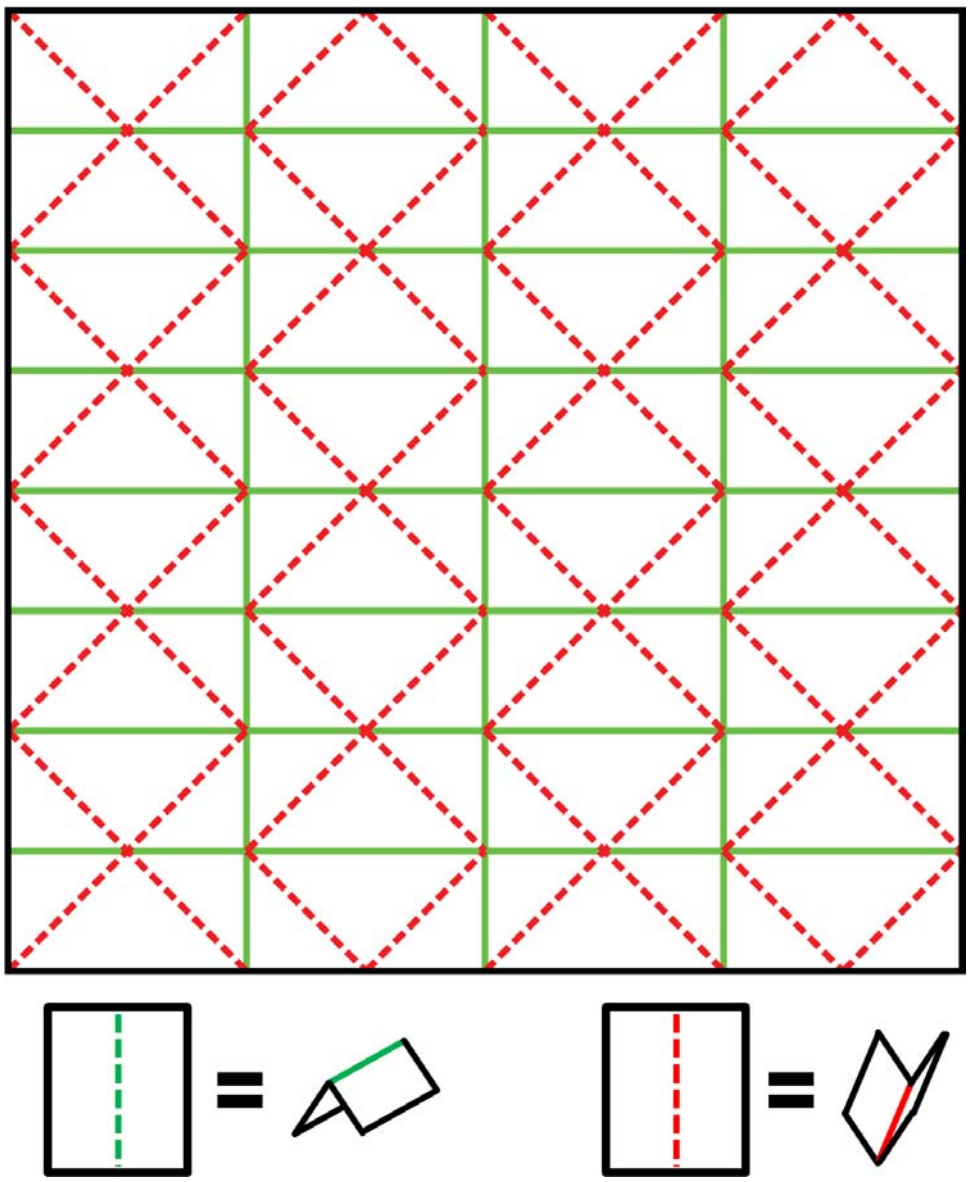

Figure S6: Origami Designs: Crease pattern for the fabrication of a multiwell plate. Mountain and valley folds are indicated by solid green and dashed red lines, respectively. The mechanical flexibility of the omniphobic paper allowed us to form 3-D structures by folding the sheet of paper before or after functionalization.

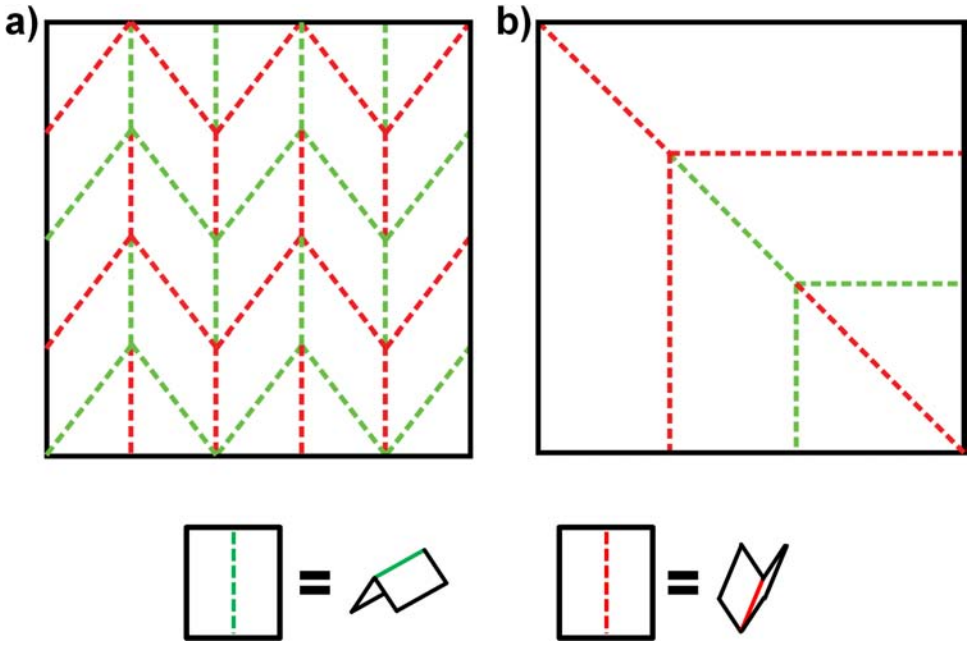

Figure S7: Origami designs for paper SLIPS: Crease pattern for the fabrication of channels and switches. Mountain and valley folds are indicated by green and red dashed lines, respectively. The mechanical flexibility of the omniphobic paper allowed us to form 3-D structures by folding the sheet of paper after impregnation with a perfluoropolyether (Krytox® GPL105).

Estimation of the Surface Free Energies of the Functionalized Papers. The method developed by Owens–Wendt–Rabel–Kaelble allows us to calculate the polar and disperse components of the surface energy and uses a geometric mean of these in the expression for γ_{LA}. We estimate the surface energy of the different R^F and R^H modified papers using the geometric mean equation:

$$(1+\cos\theta_{app})\,\gamma_{LA} = 2[(\gamma_{SA}^{d}\,\gamma_{LA}^{d})^{1/2} + (\gamma_{SA}^{p}\,\gamma_{LA}^{p})^{1/2}] \quad (1)$$

θ_{app} is the static apparent contact angle, and γ_{SA} and γ_{LA} are the interfacial free energies with air of the solid and liquid, respectively. The superscripts *d* and *p* refer to the dispersive and polar components of surface energy, respectively.

By solving Equation (1) for diiodomethane and pure water as test liquids, we obtained total apparent surface free energies between 7 and 11 mN/m for surfaces treated with the fluoroalkyl silanes, below the 18-20 mN/m reported value for polytetrafluoroethylene (PTFE). Based on the typical values for surface energies of exposed -CF_2- (18mN/m) and -CF_3 (6 mN/m) groups,[1, 2] the calculated values for the surface free energies of fluorinated paper would indicate a high ratio of CF_3 groups to exposed CF_2 groups. The trend corresponds to what is expected from the chemical nature of the surface.

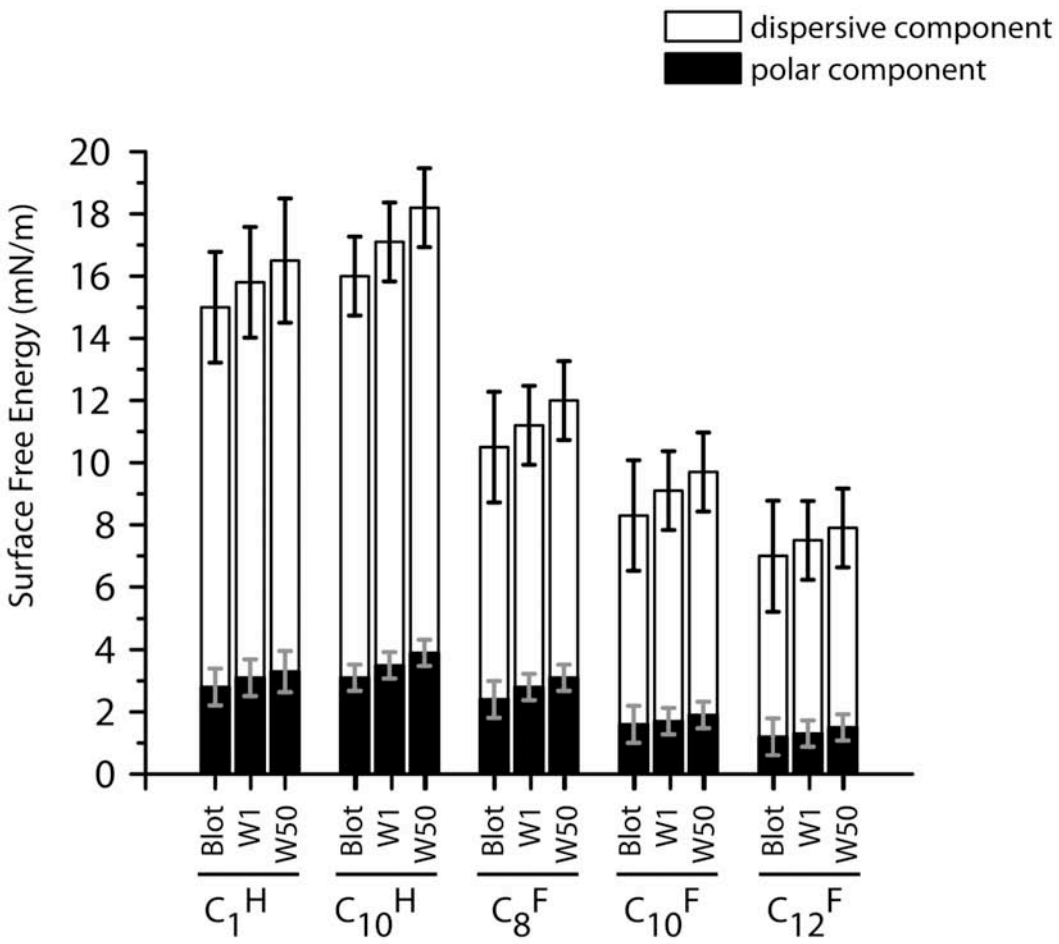

Figure S8: Dispersive and polar components of the apparent surface free energy for Gel Blot paper (Blot), Whatman #1 (W1) and Whatman #50 (W50) paper functionalized with alkyl trichlorosilane (C_1^H and C_{10}^H) and fluoroalkyl trichlorosilane (C_8^F, C_{10}^F and C_{12}^F). Error bars represent standard deviation (N=30).

Disposability of the fluorinated paper surfaces: estimate of products formed upon incineration. Combustion of fluoroalkanes occurs at temperatures above 1500°C [3-6] under atmospheric pressure. The distribution of products includes COF_2, CF_4, CO, and CO_2,[4] with COF_2 and CO_2 being the most abundant when the combustion occurs with 20% O_2.[3, 4] The toxic volatile compounds, COF_2 and HF, have threshold limits for short-term exposure of 2ppm (5.4 mg/m^3) for COF_2 and 2 ppm (1.7 mg/m^3) for HF.

We used a FLIR (Forward Looking Infrared) camera (B400, FLIR Systems Inc.) to record the burning of paper with different surface treatments, and recorded the maximum temperatures in each individual image. In the case of untreated paper, paper treated with C_1^H, and paper treated with C_{10}^H, the maximum temperatures are ~ 630°C between ~ 670°C, respectively. In the case of paper functionalized with C_8^F, C_{10}^F and C_{12}^F, the maximum temperatures are between ~ 450°C and ~ 490°C. The R^F papers burned more slowly, and generated flames of lower temperatures, than untreated paper and R^H paper.

If the R^F paper is burned in a simple set-up, with no high-temperature combustion catalyst present in the system when the paper is burned, the temperature of the flame is likely not high enough to allow the decomposition of the fluoroalkyl chains. It is, however, sufficiently high [7] to allow the breaking of the C-Si bond and the oxidation of the terminal carbon atom to yield terminally oxidized fluoroalkyl species.

The amounts of perfluoroalkylcarboxylic acid, HF and COF_2, released as by-product upon burning paper functionalized with C_{12}^F are estimated based on the elemental analysis (wt % C, F, Si) performed by the Intertek QTI Laboratory (Whitehouse, NJ). The results of the elemental analysis are summarized in Table S1.

Table S1: Elemental analysis (wt%) of papers functionalized with C_{12}^F

Type of paper	Basis weight (mg/cm²)	wt % C	wt % F	wt % Si
Whatman #50	~9.3	42.7 ± 0.3	0.5 ± 0.5	0.0018 ± 0.0005
Whatman #1	~8.6	42.8 ± 0.3	0.6 ± 0.5	0.0019 ± 0.0005
Gel Blot paper	~49.3	42.3 ± 0.3	0.6 ± 0.5	0.0041 ± 0.0005

We can estimate, based on the Si content, that one cm^2 of Gel Blot paper functionalized with C_{12}^F contains $\sim 7 \times 10^{-8}$ moles C_{12}^F, corresponding to $\sim 4 \times 10^{16}$ molecules C_{12}^F per cm^2 of paper. Similarly, one cm^2 of functionalized Whatman #1 and Whatman #50 papers contain$\sim 6 \times 10^{-9}$ moles or $\sim 4 \times 10^{15}$ molecules C_{12}^F per cm^2 of paper.

Thus, the incineration of 1 cm^2 of Gel Blot paper functionalized with C_{12}^F will produce at most 34 μg of perfluoroalkylcarboxylic acid ($C_{12}H_3F_{21}O_2$), corresponding to a maximum of ca. 29 μg of HF, or a maximum of ca. 49 μg of COF_2. The amounts of fluorinated products released by the incineration of 1 cm^2 of Whatman #1 and Whatman #50 papers are maximum ca. 3 μg of perfluoroalkylcarboxylic acid, or ca. 2.6 μg of HF and ca. 4.3 μg of COF_2.

Cost of materials. An average of 12 sheets of 20 cm x 25 cm paper can be functionalized during one silanization experiment, conducted in a chamber with a volume of 0.01 m^3 at a temperature set at 95°C. Each experiment typically required approximately 100 mg of organosilane in 10 mL of anhydrous toluene. The cost of one 20 cm x 25 cm sheet of Whatman#1 paper is ~$0.27, making the cost of 1 m^2 Whatman#1 paper ~$5.4.

Table S2: Cost of silanizing reagents as purchased at laboratory scale

Organosilane	C_1^H	C_{10}^H	C_8^F	C_{10}^F	C_{12}^F
Cost of 100 mg reagent ($)	0.05	0.18	0.27	0.35	0.47
Cost reagent ($/m²)	0.08	0.30	0.45	0.58	0.78

References

[1] A. W. Adamson, A. P. U. Gast, *Physical Chemistry of Surfaces*, Wiley, **1997**.

[2] T. Nishino, M. Meguro, K. Nakamae, M. Matsushita, Y. Ueda, *Langmuir* **1999**, *15*, 4321.

[3] E. A. Fletcher, D. Kittelso, *Combust. Flame* **1968**, *12*, 164.

[4] C. H. Douglass, H. D. Ladouceur, V. A. Shamamian, J. R. McDonald, *Combust. Flame* **1995**, *100*, 529.

[5] L. E. Fuller, E. A. Fletcher, *Combust. Flame* **1969**, *13*, 434.

[6] R. A. Matula, D. I. Orloff, J. T. Agnew, *Combust. Flame* **1970**, *14*, 97.

[7] R. L. Schalla, *UNT Digital Library* **1954**, Doc. ID:19930087991.